

We are IntechOpen, the world's leading publisher of Open Access books Built by scientists, for scientists

6,900

Open access books available

186,000

International authors and editors

200M

Downloads

Our authors are among the

154

Countries delivered to

TOP 1%

most cited scientists

12.2%

Contributors from top 500 universities



WEB OF SCIENCE™

Selection of our books indexed in the Book Citation Index
in Web of Science™ Core Collection (BKCI)

Interested in publishing with us?
Contact book.department@intechopen.com

Numbers displayed above are based on latest data collected.
For more information visit www.intechopen.com



Fianite in Photonics

Alexander Buzynin

*A. M. Prokhorov General Physics Institute, Russian Academy of Sciences
Russia*

1. Introduction

The further progress in photonics, as well as in many other technological fields is connected with application of new materials. Fianite is the material of such kind. Fianites are single crystals of zirconia- or hafnia-based cubic solid solutions with yttrium, calcium, magnesium or lanthanides (from gadolinium to lutetium) stabilizing oxides ($ZrO_2(HfO_2) \cdot R_2O_3$, where R - Y, Gd ... Lu). Industrial technology of synthesis of fianite has been for the first time developed in Russia in the Lebedev Physical Institute of the Russian Academy of Sciences (FIAN in Russian), as has entitled crystals[1, 2]. Serial production of the crystals has been already started in the early seventies of XX century [3-5]. Currently, fianite crystals are in the second position by the volume of worldwide production following silicon. Fianite single crystals - zirconia-based solid solutions (or "yttrium stabilized zirconia" - YSZ) are widely known worldwide as jewelry material (fig. 1).



Fig. 1. Great color variety of the crystals combined with unique optical properties makes fianite single crystals a promising material for jewellery, arts and Crafts (left); fianite substrates 3" in diameter (right).

Recently, in the countries with the developed microelectronics a significant growth of interest to various aspects of fianite application in semiconductor technologies has been observed. Fianite is an extremely promising multipurpose material for new optoelectronics technologies due to its unique combination of physical and chemical properties. It can be used in virtually all of the main technological stages of the production of micro-, opto- and SHF-electronics: as a bulk dielectric substrate, a material for buffer layers in heteroepitaxy; a material for insulating, antireflection, and protective layers in the devices and as a gate dielectric [6-22].

The use of fianite, as well as ZrO_2 and HfO_2 oxides instead of SiO_2 as gate dielectrics in CMOC technology, which can be considered for microelectronics as a basic one, is of peculiar interest [14, 15]. That is associated with the increase of leakage currents by the increase of the integration level when conventional SiO_2 is used. Therefore, a change of SiO_2 over dielectrics with higher values of dielectric constant (high-k-materials) is required. Due to higher value of dielectric constant (25÷30 for fianite [4, 14, 15] instead of 12 for SiO_2) it is possible to provide the same electric capacity using much more thick layers of the gate oxide.

A number of modern aspects of the application of fianite in photonics are analyzed in this chapter.

2. Techniques for the synthesis of fianite crystals

Fianite substrates

Peculiarities of the synthesis, the investigation techniques and properties of the crystals have been considered in details in [3-5]. In this chapter only brief information concerning synthesis of the crystals and manufacturing the substrates is presented. A novel laser technique developed for instant monitoring of defects in the substrates and in bulky fianite and sapphire crystals is also considered

2.1 Crystal growth of fianites using installations with cold containers of 130-700 mm diameter

The growth technique of the crystals was elaborated and developed using following installations: "Crystal -407" (5.28 MHz frequency, 60 kW power, ØCC 130mm); "Crystal -403" (1.76 MHz, 160 kW, ØCC 400mm); "Crystal -403M" (0.4-0.88 MHz, 600 kW, ØCC 700mm) (Fig.2).

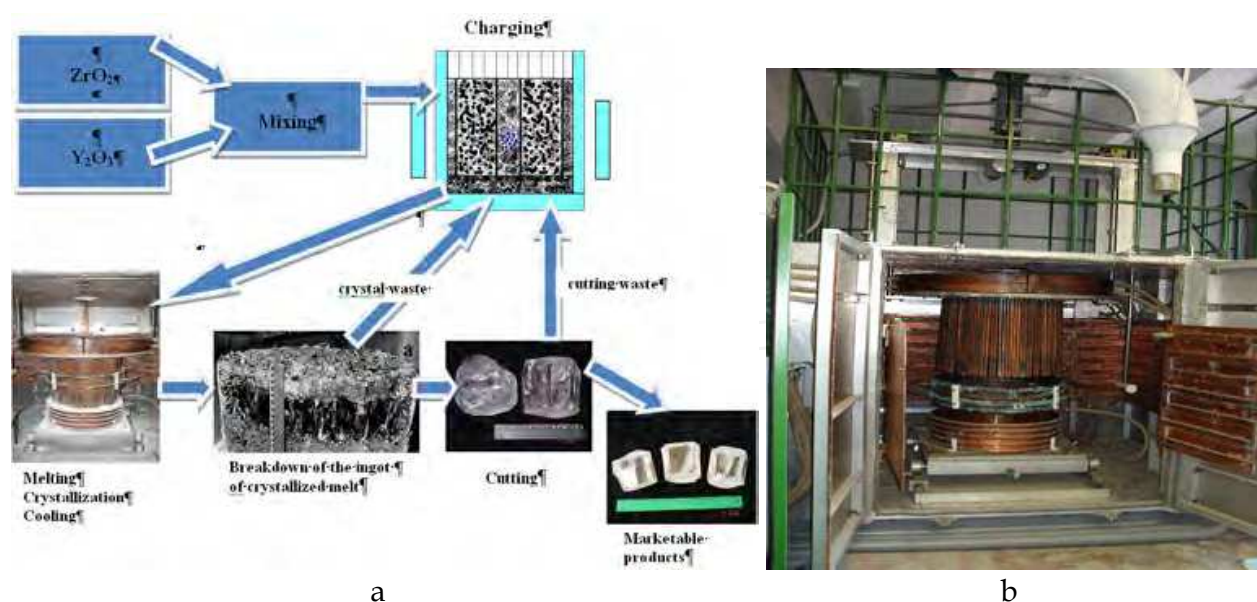


Fig. 2. The scheme of manufacturing of zirconia-based crystals (a); Installations for direct RF melting of dielectric materials in a cold container (CC) "Crystal -403M" (0.4-0.88 MHz frequency, 600 kW power, ØCC 700mm) (b).

2.2 Technology for mechanical machining of fianite crystals

Fianite lend itself to a machining considerably readily, similarly to sapphire crystals. Dislocation densities in $ZrO_2 - (8-20) \text{ mol\% } Y_2O_3$ crystals have been measured:

in central parts - 10^3 cm^{-2}
in periphery - 10^5 cm^{-2}

Followed by annealing (2100°C , vacuum) dislocation density decreased to $10^2 - 10^3 \text{ cm}^{-2}$.

Pre-epitaxial treatment of surface of the substrates. With the purpose to guarantee optimal physical-chemical state of fianite substrates various techniques and conditions of pre-epitaxial treatment have been studied. Treatment at $1000-1400^\circ\text{C}$ temperatures in air during 1-4 h was used as one of such techniques. The high-temperature annealing provides a relief of stress occurred in the surface layer at mechanical treatment, removal of impurities from the surface and increasing of phase and structural perfection.

The effect of high-temperature annealing on surface quality of the substrates has been studied. In Fig.3a scratches occurred in course of polishing of the substrate by ACM 1/0 diamond paste are apparently observable. The following annealing (1250°C in air) did not result in smoothing of the relief as a whole but caused re-structuring of the surface layer (Fig. 3b) and flatten the relief in micro-locations at scratch residues and results in 2-3-fold decrease of high bump- valley drops (Fig. 3, right side)

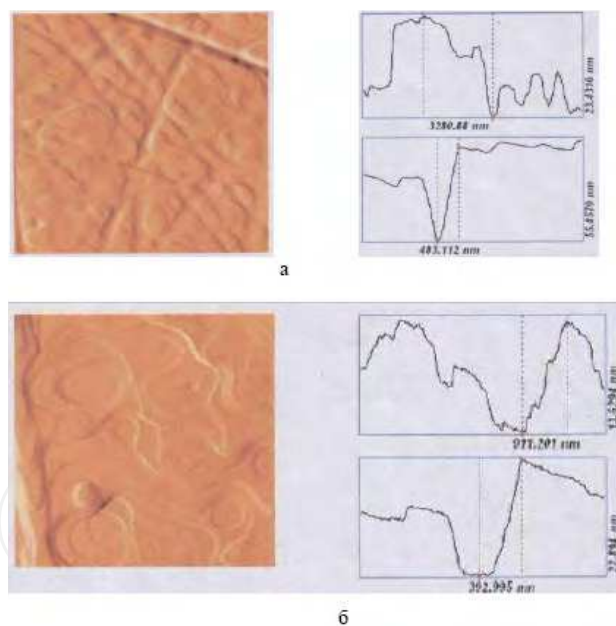


Fig. 3. AFM image of fianite substrate (left) and surface profile (right) after chemical-mechanical polishing (a) and subsequent high temperature annealing (b).

The studies of the effect of thermal treatment of the substrates on roughness of polished surface have shown that high-temperature annealing ($1250-1400^\circ\text{C}$) conducted following chemo-mechanical treatment promoted an increase of structural and phase homogeneity of the surface of zirconia-based crystal substrates.

Half-width of the rocking curve (HWRC) is another parameter featuring quality of a substrate surface. The HWRC values significantly decreased due to the annealing.

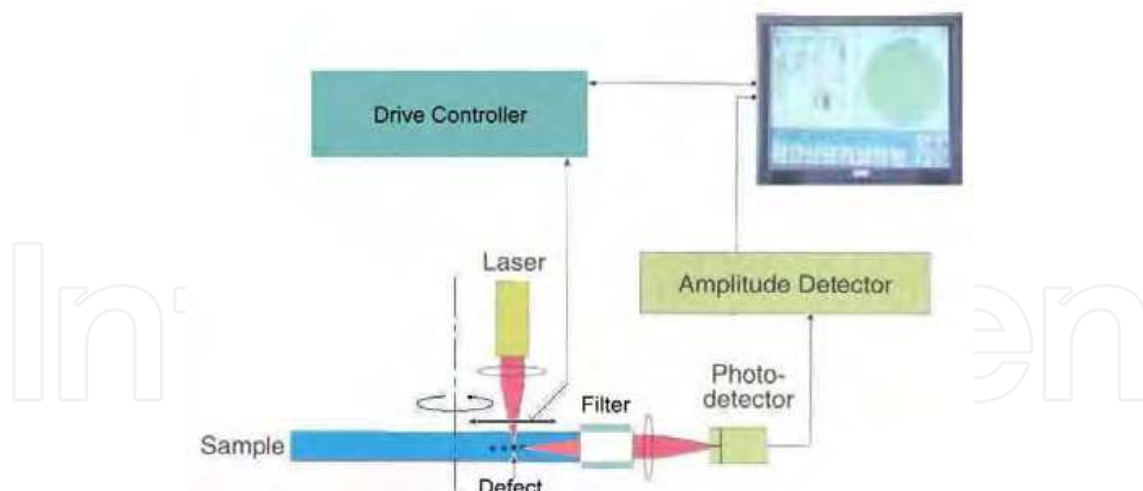


Fig. 4. Draft-scheme of the apparatus for laser control of sapphire and fianite wafers and bulky crystals

The technique for production of epi-ready substrates has been developed. The epi-ready substrates of 2" and 3" diameter have been manufactured from zirconia-based crystals. The polished surface was mirror-flat, scratches, etching pits, fractures and other defects are absent. The profilograms showed no noticeable deviations from $R_2 - 5$ nm height. Typical roughness σ values for the epi-ready polished surface of fianite are less than 0.5 nm.

2.3 New laser technique for express-monitoring of the defects in a volume of wafers and crystals - Development of the technique and equipment

The Laser technique is based on a laser emission at the wavelength, which coincides with the region of transparency of sapphire and fianite, for example, radiation of CO₂-laser in the middle IR range ($\lambda \sim 5.4 \mu\text{m}$).

Such laser radiation readily penetrates through the flawless regions of fianite and sapphire, and scatters on impurity inclusions within fianite volume and micro-bubbles within sapphire volume. The scattered part of radiation passes through the filter and is registered by a photodetector arranged perpendicularly to the direction of the laser beam. Subsequent computer processing of the signal provides information on the defects.

Besides information on presence or absence of the defects in a volume of wafers and crystals, it is also possible to observe its two- or three-dimensional distribution over square of a plate and volume of a crystal.

This technique allows:

- monitoring of all defective wafers and separating really defective wafers with micro-bubbles (typical defects of sapphire) and impurity inclusions (typical defects of fianite) from tentatively defective ones with surface defects only, those which may be relieved by special treatment (thus increasing the yield);
- selecting defective segments in the bulk crystals for the most economic scribing.

The data obtained can be sorted and saved in a computer memory for the subsequent analysis of reasons of the defect formation in bulk crystals with the purpose of the technology improvement.

The laser technique has the following advantages. It is: contactless, nondestructive, express, rather easily automated, technological and easy in use. So it is convenient for the use in commercial production with hundred percent inspections of the products and for the solution of some scientific and technological problems.

Development of the laser control equipment. Draft-scheme of apparatus for laser control of sapphire and fianite wafers and bulky crystals is shown in Fig. 4.

The laser control apparatus has the following characteristics:

- Apparatus sizes are - 1m x 1m x 1.5 m;
- Wafer diameter - from 0 up to 2" (can be increased up to 6" and more);
- Wafer width 0.5 - 3 mm and more, bulk crystals height up to 20 cm and more;
- The surfaces can be polished, finely ground or roughly ground;
- Time for the test of one substrate (slice) with 2" diameter is less than 10 seconds, 6" - about one minute.

Fast horizontal scanning of the whole wafer is provided by its rotation and the radial movement of the light from motionless laser (the optical system is used). At tomographic investigations of bulky crystals a periodical crystal movement along vertical axis with a given step (for example 0.5 or 1 cm) is added.

Operational characteristics of the apparatus can be further improved [23, 24].

3. Fianite as a substrate and buffer layer for Si, Si-Ge and A^{III}B^V compounds epitaxy

Fianite has a number of advantages over other dielectric materials as a substrate and buffer layer for the epitaxy of Si and A^{III}B^V compounds [6-12, 16-18].

A wide spectral range (260–7500 nm) of the fianite transparency completely covering absorption and emission ranges of A^{III}B^V compounds and its solid solutions makes "semiconductor-on-fianite" structures promising for the development of various optoelectronic devices with advanced characteristics, including photodiodes with Schottky barrier, photoresistors, emitting and laser diodes, avalanche photodetectors.

Thin films of fianite and related solid solutions such as Zr(Ce)O₂ can be used as **insulating layers** (alternative to SiO₂, SiC, Si₃N₄) in development of Si-, Ge- and GaAs-based "semiconductor-dielectric" multilayer structures. Fianite is also good **gate dielectric** for Si- as well as for A^{III}B^V -based devices (including GaN-based) due to its high dielectric constant value (25...29.7). Thin fianite films are a barrier for diffusion of impurities and provide significant (up to 1000-fold and even more) decrease of current loss in highly-integrated devices [14, 15]. Due to high chemical inertness fianite films can also be used as **protective coatings**.

The first epitaxial Si films on YSZ were grown in [6]. The first successful results on epitaxial MOCVD growth of various A^{III}B^V compounds (GaAs, InAs, InGaAs, AlGaAs, GaAsN and GaN) on YSZ are presented in a number of studies [10, 16, 17], InN on YSZ - in [21, 22]. In [17, 18] «capillary epitaxy technique» - the new effective way of heteroepitaxy - was developed. It has been shown that the use of capillary forces in the method positively influences both on the mechanism of epitaxial growth, and on

quality of $A_{III}B_V$ epitaxial films, and also reduces the minimum thickness of a continuous layer [17, 18].

An application of fianite as either monolithic substrate or buffer layer in “semiconductor-on-dielectric” technology is of peculiar importance for micro- and opto-electronics. The technology allows improving such characteristics of integrated circuits as operation speed, critical operational temperature and radiation resistance. Due to a decrease of loss of current and stray capacitance energy consumption of the devices is decreasing. Moreover, the devices based on “semiconductor-on-dielectric” structures are more reliable, especially under extreme operational conditions. Currently, “silicon-on-insulator” structures are one of the most dynamically developing directions in the field of semiconductor material science. However, electrophysical and operational parameters of the devices, as well as its radiation resistance and reliability significantly suffer because of structural imperfection of silicon layers. In case of “silicon-on-sapphire” structures the imperfection is determined, in particular, by a difference in crystallographic structure of silicon and sapphire, as well as by autodoping of a silicon film by aluminum penetrating from the sapphire substrate in concentrations up to 10^{18} – 10^{20} cm⁻³. Considering crystal-chemical and physical characteristics of fianite, the material is more preferential for the epitaxy of Si as an alternative substrate in comparison with sapphire.

In comparison with the other dielectrics, there are the following merits of fianite in application as a **substrate material and buffer layer** for Si and $A_{III}B_V$ compounds epitaxy:

- High resistivity - $>10^{12}$ Ohm•cm at 300 K;
- Similarly to Si, Ge and $A_{III}B_V$ compounds it is of cubic structure (in contrast to hexagonal of sapphire) and has low mismatch by its lattice parameters with these compounds. In particular, the mismatching of fianite (15% Y_2O_3) with silicon is $\sim 5,3$ % (Fig. 5);
- it is possible to alter fianite cubic lattice constant in solid solutions by varying ratio of the main (zirconium or hafnium dioxide) and stabilizing oxides (yttria, rare earth oxides from gadolinium to lutetium and alkaline-earth oxides) that allows an optimum matching between substrate and cubic lattice of semiconductor films thus improving its structural perfection. For example, the values of lattice parameter mismatching between Si and fianite crystals of $(ZrO_2)_{100-x} \times (Y_2O_3)_x$ compositions are 5.7, 5.3% and 4.4% at $x = 9, 15$ and 21, respectively;

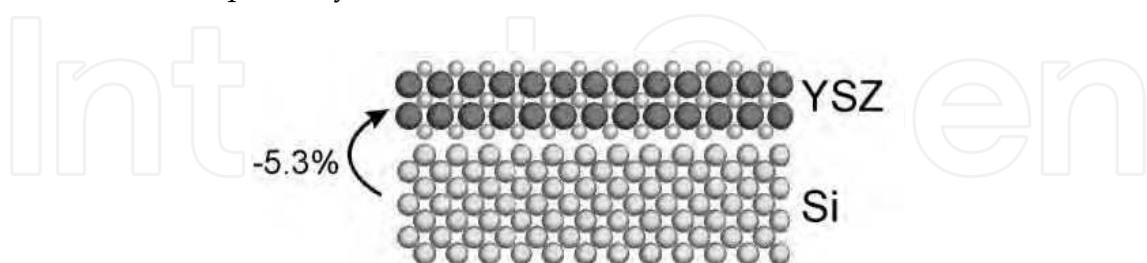


Fig. 5. Correlation of the lattice parameters of Si and fianite $(ZrO_2)_{0,85} \cdot (Y_2O_3)_{0,15}$.

- Fianite is characterized by low cation diffusion up to 1000–1200°C temperatures that reduces interdiffusion of substrate and film impurities and uncontrollable self-doping of a film (typical for sapphire) hindering the film parameters;
- Due to its excellent stability at elevated temperatures, the upper limit of the corresponding structure operational temperatures depends on physical properties of a semiconductor only. Elevated temperature is not critical for the substrate.

- Fianite is very promising material for the development of semiconductor-on-fianite structures for various optoelectronic devices with enhanced characteristics. It has broad band of optical transparency (260 to 7500 nm), which completely overlaps the absorption and emission bands of Si and A^{III}B^V compounds and their solid solutions
- Application of thin layers of fianite on Si and GaAs instead of its monolithic substrates allows avoiding spatial limitations of the structures and decreasing the net cost. At the same time, the structures on “fianite/Si” and “fianite/GaAs” episubstrates have better heat conductivity in comparison with the structures on monolithic substrates.

3.1 Silicon-on-fianite epitaxial structures

The first studies on silicon epitaxy on fianite single crystal substrates have been carried out in France and USA [7, 8]. Silicon films on fianite substrate were deposited by chloride and hydride epitaxy at 900...1100°C. The films obtained were of polycrystalline structure and, consequently, featured with poor electrophysical parameters. However, at the same time it was shown that silicon-on-fianite structures sustaining actually all advantages of silicon-on-sapphire are free from its principal drawbacks.

At the epitaxy of Si on fianite a formation of SiO₂ intermediate layer between the film and the substrate was observed [7, 8]. Subsequent annealing of the structure led to the increase of SiO₂ layer thickness. It was demonstrated [8] that the layer can improve properties of silicon-on-fianite epitaxial structure because its formation:

- Removes mechanical stress in the layer-substrate interface;
- Smoothens over negative effect occurring due to a difference of linear expansion coefficients between fianite and silicon;
- Improves insulation of the integrated circuit elements (ICE) based on Si;
- Acts as a barrier for metal impurities diffusing from the substrate and forming deep levels in silicon;

The formation of SiO₂ intermediate layer at high-temperature epitaxy is associated with peculiar properties of fianite. In contrast to the other dielectrics, fianite features with a unique peculiarity as a solid electrolyte: starting from 650°C it becomes actually oxygen-transparent due to high mobility of oxygen. The reason for significant mobility of oxygen in fianite crystals is an occurrence of oxygen vacancies due to Zr⁴⁺ to Y³⁺ cation substitution at formation of the solid solution. High mobility of oxygen in fianite crystals is determined by an occurrence of oxygen vacancies at ZrO₂(HfO₂) - R₂O₃ (here: R - Y, Gd...Yb) solid solutions formation due to Zr⁴⁺(Hf⁴⁺) to R³⁺ cation substitution. The process results in the oxygen non-stoichiometric ZrO₂(HfO₂) based phase [4]. Because of high mobility of oxygen at high-temperature epitaxy (900...1000°C), which was used in [6-8] the formation of either SiO₂ continuous layer or its islets between the substrate and the film was shown to be inevitable.

The phenomenon occurs even at the epitaxy initial stages when a continuous epitaxial film is forming. It was shown [9] that the formation of SiO₂ layer or isles at the initial stage of molecular-beam epitaxy on fianite results in 3-dimensional mechanism of growth, formation of structural defects and hindered the synthesis of Si films of single crystal structure. The occurrence of oxide SiO₂ isles at the initial epitaxy stages and polycentric growth of Si layers were shown possible to avoid only by using a set of techniques, those which prevent diffusion of oxygen from the substrate to the film at initial stage of the process. In particular,

high structural perfection of the Si-on-fianite films was achieved by using low-temperature ($T < 650^\circ\text{C}$) molecular-beam epitaxy [9].

3.2 Ge and GeSi films on fianite substrates

Growth of Ge and Ge-Si heterostructures on fianite substrates was carried out using the installation shown in Fig. 6.

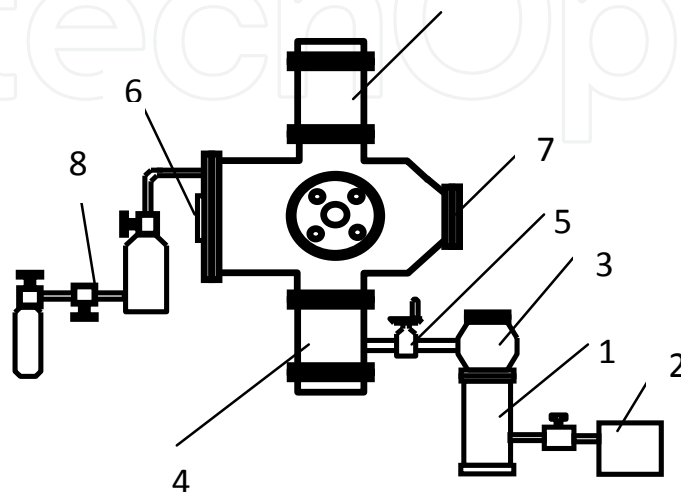


Fig. 6. Draft-scheme of *HWCVD* installation for $\text{Si}_{1-x}\text{Ge}_x$ growth: 1 - diffusion pump, 2 - forepump, 3 - liquid nitrogen trap, 4 - getter-ion pump, 5 - high-vacuum shuttle, 6 - charging flange for sources, 7- charging flange for substrate, 8 - system for supply of GeH_4

The growth cell comprised a stainless steel cylinder of 290 mm inner diameter and 360 mm length. There were two charging flanges in the cylinder faces, one for 3 pairs of current leads and the other for current leads for a substrate.

Base pressure in the chamber $\sim 1 \cdot 10^{-8}$ torr was maintained by pump-down using two hetero-ionic pumps. High-vacuum gate was used for isolation of the growth cell and the pumps from other parts of the vacuum system. Forepumping of the chamber was performed using diffusion pump. The diffusion pump allowed to exhaust any gas (including GeH_4) both in atomic and molecular state. FM-1 oil with low vapor pressure was used as a pressure fluid. There was a nitrogen trap above the diffusion pump preventing reverse diffusion of the oil from preevacuation and diffusion pumps into the growth cell. The (100) and (111) oriented fianite single crystal plates were used as substrates. Silicon atomic beam was maintained by sublimation of the element single crystal (high-resistance) in form of $4 \times 4 \times 90$ mm ingot sections. The sources were mounted on the cooled current leads. There was Ta plate of $80 \times 5 \times 0,5$ mm size installed in one of the sources position.

Before the epitaxial growth the sources and substrates were subjected to 10 min annealing at 1350 and 1250°C , respectively, then temperature of the source was increased to 1380°C , as the substrate temperature was decreased to assigned values (600 - 700°C) and the buffer layer was grown. The pressure in the cell corresponded to basic one.

In order to grow Ge layers the cell was filled with GeH_4 up to $1 \cdot 10^{-3}$ - $5 \cdot 10^{-6}$ torr, the pressure was maintained constant by a system of the gas feeding. Simultaneously the Ta plate

situated in vicinity of the substrate was heated to $T = 1200^\circ\text{C}$. With the purpose to avoid destruction of germane on evaporators (Ti) following pre-epitaxial annealing of the sources and substrates the sublimating pumps were switched off and the growth was carried out at pumping-down using only diffusion- and for-pumps. It is worth to note that the gas filling up to such high pressure ($\sim 10^{-3}$ torr) is impossible in MBE installations with electron-beam heating. The pressure in the cell was tentatively assigned by ionization vacuum gage indications. Nevertheless, this peculiarity in GeH_4 pressure measurement did not impede the controlled growth of Ge films at $700\text{-}750^\circ\text{C}$ temperature of the substrate. Ge films were continuous and homogeneous. Solid solution GeSi with up to 80% Si content on fianite substrates (111) and (100) also was obtained. Vacuum annealing at 1250°C during 10 min was used as pre-epitaxy treatment. The growth was carried out under $5 \cdot 10^{-4}$ torr germane pressure and at 600°C substrate temperature. Simultaneously, Ta plate positioned in vicinity of the substrate was heated to 1200°C . At fig. 7 X-ray diffraction pattern of Ge film ($0.3 \mu\text{m}$ thickness) on fianite substrate (111) is shown, $\text{Ge}(111) 27.3^\circ$ and $\text{YSZ}(111) 30.0^\circ$ peaks are apparent. Heteroepitaxial Ge films obtained show high structural perfection. The half-width of the X-ray curve for Ge film of $0.3 \mu\text{m}$ thickness was 0.31° (fig. 7).

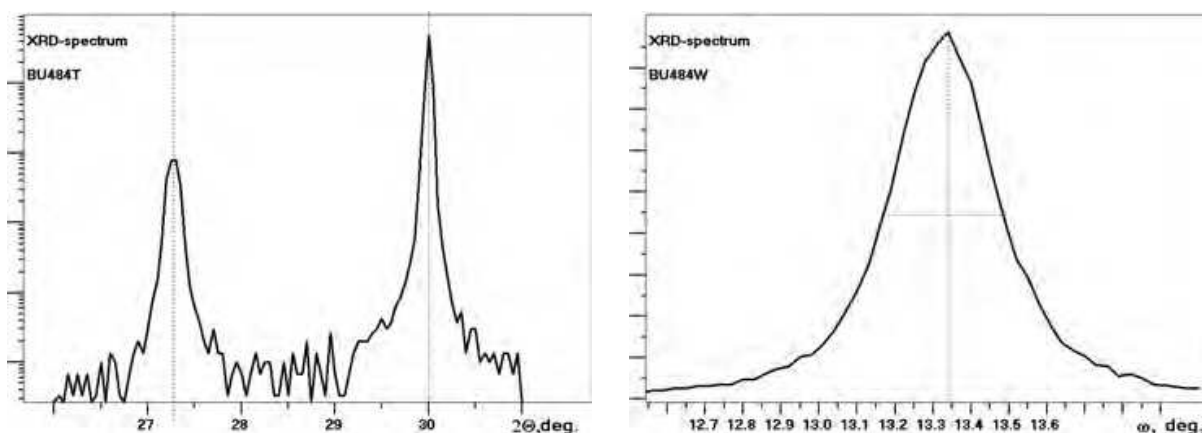


Fig. 7. Spectra of $\theta/2\theta$ - scanning (a) and rocking curve (b) of Ge layer on (111) fianite.

The surface morphology of the Ge epitaxial layers grown on (100) and (111) fianite substrates (fig. 8a) as well as the peaks of Raman scattering near 300 cm^{-1} (fig. 8b) are identical to those of bulk Ge. Therefore, it is possible to conclude that there are no stains in the Ge/fianite layer.

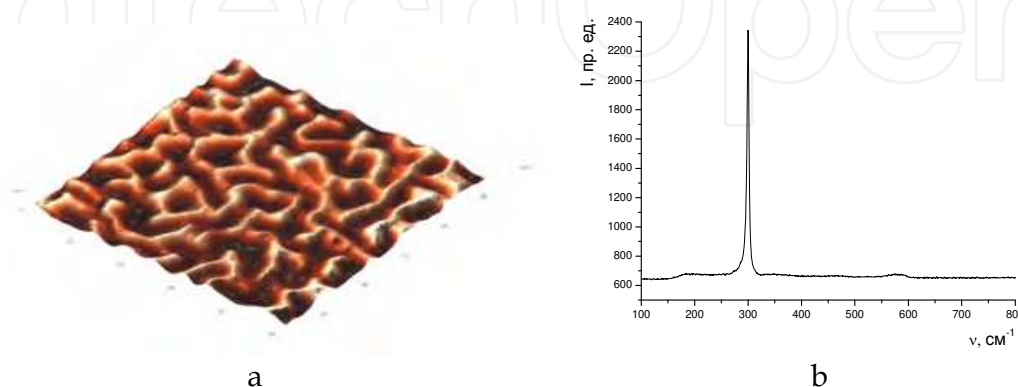


Fig. 8. Surface morphology (a) and Raman spectrum (b) of Ge film on fianite; $T_s=700^\circ\text{C}$, $t=60 \text{ min}$ (AFM).

3.3 Epitaxial films of A^{III}B^V on-fianite

Crystallochemical and physical properties of fianite are favorable not only for silicon but also for A^{III}B^V compounds epitaxy (Table 1).

Crystal	Lattice		T _m , °C (melting point)	Therm.Exp.Coeff. 10 ⁻⁶ deg ⁻¹	E _g , eV
	type	a, Å			
(ZrO ₂) _{100-x} (Y ₂ O ₃) _x	Cubic (fluorite)	5.141(x=10) 5.157(x=15) 5.198(x=21)	2800	11.4 (15-1000°C)	
GaAs	Cubic (sphalerite)	5.65	1283	5.4	1.43
GaP	Cubic (sphalerite)	5.445	1467	4.7	2.26
GaN	Hexagonal (wurtzite)	a=3.186; c=5.178	1700	5.6 ; 7.8	3.4
GaN	Cubic (sphalerite)	4.52	1700	3.9	3.2
InN	Hexagonal (wurtzite)	a=3.54 c=5.70	1200	12.7	0.7
InN	Cubic (sphalerite)	4.98	1200	4.4	0.67

Table 1. Some properties of fianite crystals and A^{III}B^V compounds.

First successful results on growth of A^{III}B^V compound epitaxial films on fianite substrates were presented in [10, 17]. GaAs, InAs, GaN and other A^{III}B^V semiconductor compound films have been grown on fianite, as well as on silicon and gallium arsenide with fianite buffer layer substrates by means of metal-organic Chemical Vapor Deposition (MOCVD). A new efficient epitaxy technique - "capillary epitaxy" has been suggested. The technique allowed synthesizing of A^{III}B^V compounds films by MOCVD on fianite substrates. Samples of structurally perfect sub-micron (up to 0.1 μ) epitaxial films of A^{III}B^V compounds have been obtained using this technique. The samples demonstrated high electrophysical parameters [16, 17, 19, 25, 26]. In [20] GaN epitaxial films have been grown on fianite substrates by MOVPE technique. It was observed that the epitaxial growth of GaN on fianite significantly depends on conditions of initial stage of the process.

In [12, 21, 22] fianite substrates were successfully tested for growth of InN heteroepitaxial films. InN films of cubic structure have been grown on (001) fianite substrates by plasma-stimulated molecular-beam epitaxy (RF-MBE) at 400-490 °C temperature. The lattice mismatch of InN and fianite at (001) plane is very low (less than 2.3%), in contrast to 17% for InN - sapphire and more than 10% for InN - GaAs. Due to this fact, InN films grown on (001) fianite substrate were superior InN films grown on sapphire [12] and (001) GaAs substrates by its crystallographic perfection [22].

Therefore fianite is apparently in advance as a substrate for InN epitaxy as compared to sapphire. A new effective method of heteroepitaxy, capillary epitaxy, was proposed in [17]. It allows us in particular to obtain films of $A^{III}B^V$ compounds on fianite using the MOCVD approach.

3.3.1 GaAs on fianite films - MOCVD capillary epitaxy of III-V on fianite

The investigations showed that continuous GaAs layers on fianite can be obtained only in a very narrow range of epitaxial conditions. In particular, temperature range of 550-600°C is necessary. The minimum thickness of a continuous layer was 1.5-2.0 μm . The epitaxial films had polycrystalline structure and rough surface. Structural and electrical properties of GaAs films could be improved using capillary epitaxy. The essence of this method is that a thin (less than 50 nm) film of an III-group element is initially deposited on the fianite surface and then saturated with a V-group component with the formation of a thin continuous epitaxial III-V layer. After this procedure, the film growth continues to obtain the necessary thickness under conventional epitaxial conditions.

The use of capillary forces in the first (heteroepitaxial) stage of GaAs film formation led to improvement of epitaxial quality. Electron microscopy of the GaAs films at the initial growth stages showed that the transition from the standard MOCVD growth to capillary epitaxy leads to a change in the growth mechanism. Three-dimensional island mechanism changes to the two-dimensional one with propagation of the growth steps (Fig. 9, A). This process is similar to graphoepitaxy [27, 28] from aqueous solutions with addition of surfactants, where an increase in the substrate wettability also significantly improves the quality of graphoepitaxial layers [27] (Fig. 9, B).

In both cases, the height of the crystallization medium (melt or solution) decreases in the initial stage due to the capillary forces. This effect impedes growth of epitaxial nuclei in the direction normal to the substrate surface and facilitates their growth in the tangential direction. As a result, the substrate orienting role increases and a transition to the layer-by-layer growth mechanism occurs with a decrease in the growth step height. As a result, the minimum height of the continuous layer decreases and the film structural quality is improved. It has been shown that the use of capillary force in this method has a positive influence on both the mechanism of epitaxial growth and the quality of $A^{III}B^V$ epitaxial films. It also reduces the minimum thickness of a continuous layer [17, 19]. Virtually the same approach has now begun to be used with success in the works of other authors in order to obtain $A^{III}N$ films on various substrates [29].

The use of capillary epitaxy made it possible to decrease minimum thickness of a continuous GaAs/fianite film to 25 nm and to improve its structural quality and surface morphology. The technique was also efficient for growing other $A^{III}B^V$ compounds on fianite.

3.3.2 Study of impurities content in GaAs-on-fianite films using mass-spectrometry analysis

Mass-spectrometry analysis using single crystal GaAs standard curve has shown concentration of the impurities in GaAs-on-fianite films grown using the capillary epitaxy technique to be in the range of $5 \cdot 10^{16}$ - $5 \cdot 10^{17} \text{cm}^{-3}$ (Tab. 2). Layerwise mass-spectrometry analysis of the GaAs/fianite structures has shown uniform distribution of the impurities in GaAs film. Somewhat increase of Ca, Na and Cr concentrations in the film-substrate interface seems to be associated with a formation of oxides in the interface.

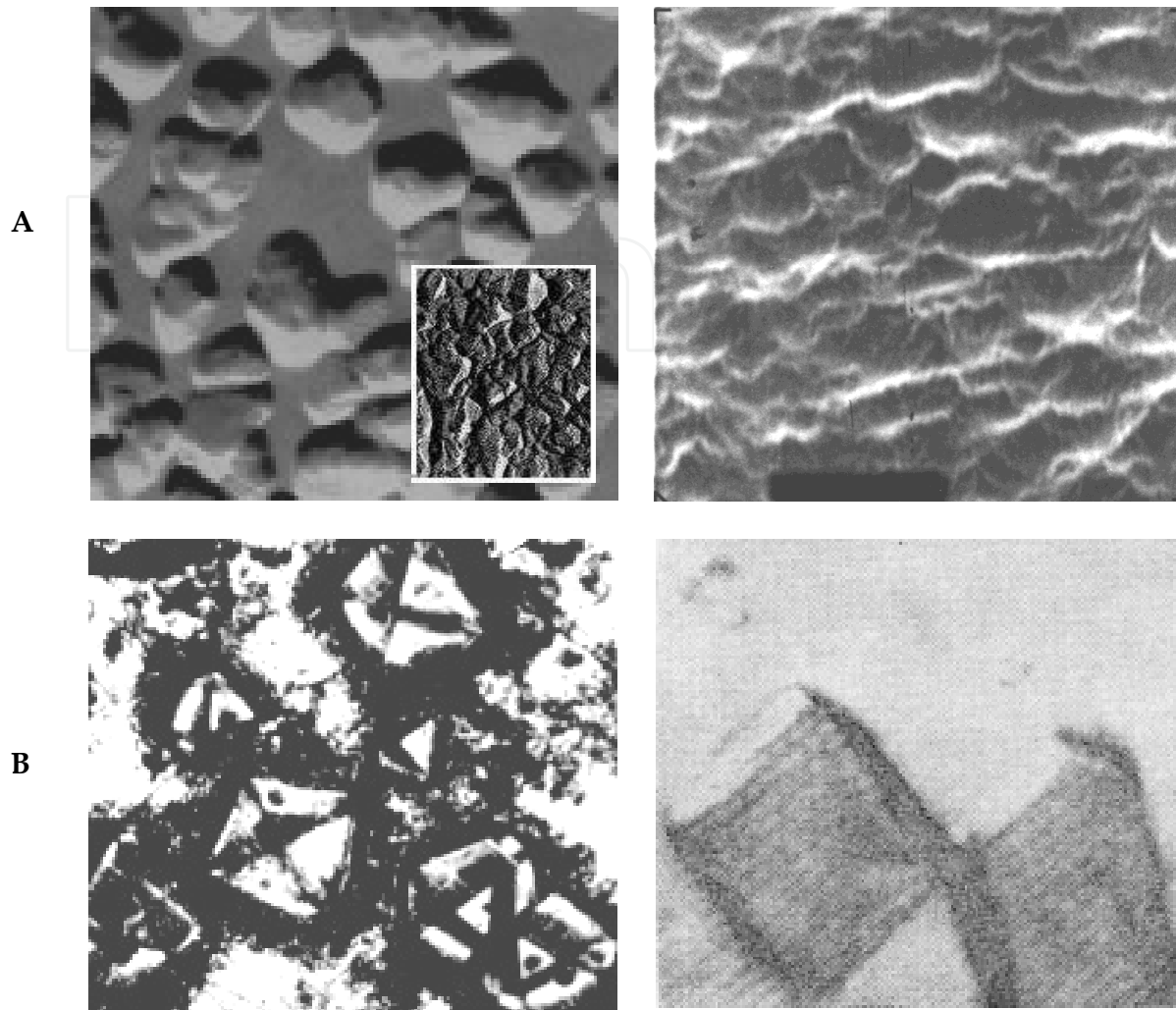


Fig. 9. Analogy between capillary epitaxy and graphoepitaxy: A - Electron microscopy image of GaAs on YSZ initial stage of growth (20000 \times): Conventional MOCVD, height of the islets is up to 3000 nm, left; Capillary epitaxy technique, minimal layer thickness is 50 nm, layers growth is visible, right [17]; B - *Optical microscopy image of NH₄I on amorphous Al graphoepitaxy growth*: without (left) and with (right) the use of surface-active substances, magnification 100 \times [27].

3.3.3 The deposition of GaAs, GaSb, GaAs: Sb films and GaSb/InAs superlattice on fianite substrates by means of laser sputtering

Our experiments have shown that the conventional “direct” growth of heteroepitaxial films InGaAs on fianite substrates resulted in the films with rough surface. So the buffer layers were elaborated to improve the results. The buffer layer must have very high structural perfection and mirror-homogeneous surface. The multiple experiments were conducted for growth of GaAs, GaSb, GaAs: Sb buffer layers on fianite (100) and (111) substrates as well as GaSb/InAs superlattice by using laser spraying. This superlattice is working as a filter which prevents the defects penetration into InGaAs film and first of all, formation of growing dislocation. Furthermore Sb is an effective surfactant [52] which significantly improves the layer morphology.

Impurity	Fianite crystal, mass%	Fianite substrate, mass%	GaAs-on-fianite film, atoms cm ⁻³
Al	0.0004	0.001	5x10 ¹⁷
Ca	0.001	0.003	5x10 ¹⁷
Mg	0.0005	0.0005	
Na	0.0001	0.003	2x10 ¹⁷
K	0.0005	0.001	5x10 ¹⁶
Si	0.001	0.015	1x10 ¹⁷
Cu	0.0005	0.0005	
Fe	0.0004	0.0004	5x10 ¹⁶
Mn	0.0001	0.001	
La	0.0006	0.006	
Cr			1x10 ¹⁶
C			1x10 ¹⁷

Table 2. Concentrations of the impurities in the crystals, fianite substrates and GaAs films

The studies have shown that it was complicated to obtain thin and homogeneous layers of A^{III}B^V compounds on fianite substrates. It may be related to rather high mismatching of the lattice parameters of fianite and A^{III}B^V compounds leading to growth according Volmer-Weber mechanism. Formation of the continuous layer occurred through 3-dimensional nuclei, their subsequent growth and joining. Low nuclei density results in formation of highly inhomogeneous rough surface that hinders subsequent formation of a flat layer. Laser sputtering technique is considered to maintain high nuclei density, so, before joining the nuclei are of sufficiently small size that promotes formation flat continuous layer.

In order to obtain flat layers laser sputtering technique was used in the study.

The Q-switched Nd laser and single crystal GaAs and InAs targets were used. The superlattices were grown by optical switching of the layer beam between the targets. Mirror-flat GaSb, GaAs:Sb layers, as well as penta-periodic InAs/GaSb superlattices of 0.15 μm total thickness were deposited using this technique.

The X-ray diffraction investigations of GaAs:Sb (111) layers on fianite (111) showed their single-crystal structure (fig. 10a). It was shown that the spectral dependence of photoconductivity of GaSb layers on fianite substrates (fig. 10b) have a maximum of photoconductivity at the edge of fundamental absorption. This effect may be due to high velocity of the surface recombination.

The width of the rocking curve for these layers as FWHM_ω [GaSb (111)] = 0.23°. The image of the surface of GaAs:Sb (0.2 μm thickness) on fianite is shown in fig. 11a. It is apparent, that the surface of the layer is mirror-flat and sufficiently homogeneous. The microrelief of the layer surface is shown in fig. 11b. According to our estimations roughness of the layer is less than 4 nm (Sq = 0.003778 μm).

In the penta-periodic InAs/GaSb superlattices of 0.15 μm total thickness grown on (111) fianite substrates electron mobility approaches to 580 cm²/ V×s.

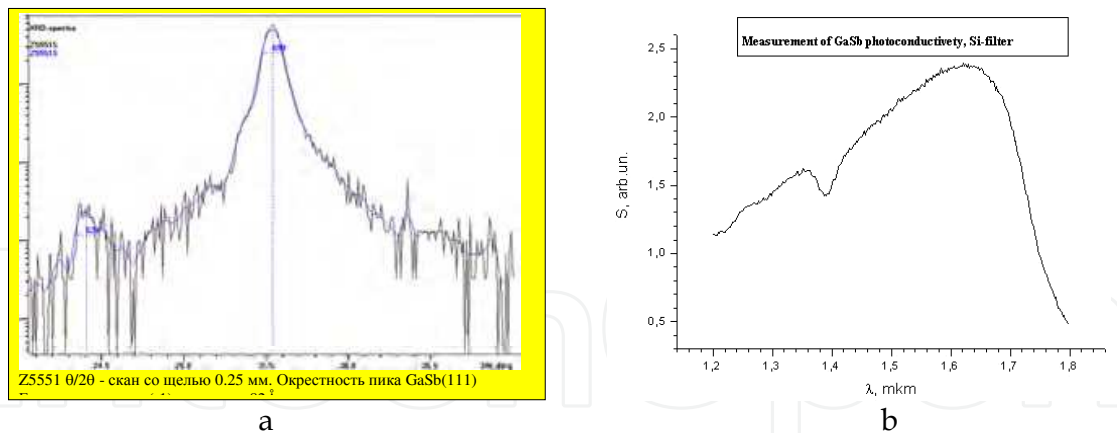


Fig. 10. X-ray rocking curve of layer GaSb(111)/fianite(111) (a); rocking curve width $\text{FWHM}\omega \text{GaSb}(111) = 0.23^\circ$; photoconductivity of GaSb on fianite substrate (b).

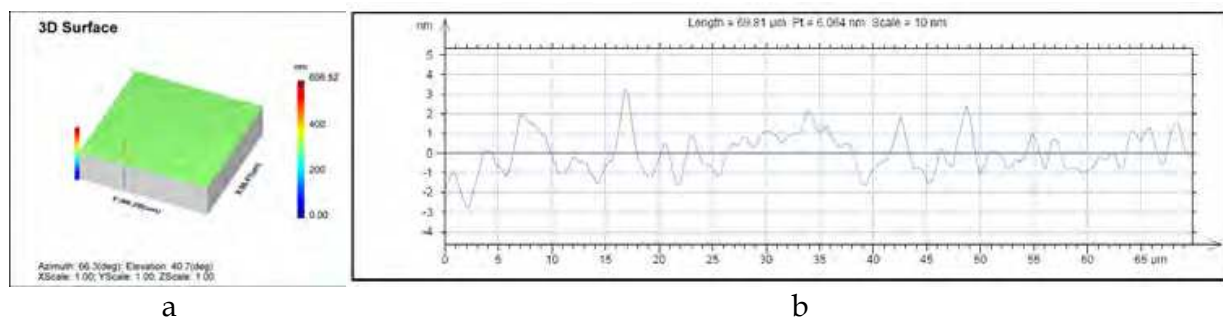


Fig. 11. Interference microscope images of surface (a) and the surface relief (b) of buffer layer GaAs:Sb on fianite (Interference microscope Talysurf).

The GaSb layers, as well as InAs/GaSb short-period superlattices are suitable for the development of IR detectors operating in 2-3 μm range. In our studies they were used as buffers for AlInN growth on fianite substrates.

3.3.4 Deposition of GaAs, AlGaAs, InGaAs – Based multilayer structures on fianite

The results on epitaxial growth of $\text{A}^{\text{III}}\text{B}^{\text{V}}$ compounds films obtained in the studies described above were used for obtaining of AlGaAs/InGaAs/GaAs multi-layer heterostructures on fianite. These structures were used in FET. Sequential growth $\text{A}^{\text{III}}\text{B}^{\text{V}}$ heteroepitaxial layers on the fianite substrates was conducted according to topologic scheme of PHEMT (Pseudomorphic High Electron Mobility Transistor) for microwave frequency FET operating in 10-40 GHz range (Tab. 3) using «Aixtron AIX 200RF» installation. Capillary epitaxy MOCVD technique in 550-600°C temperature range was used.

Grown by «capillary epitaxy» techniques series of GaSb and GaAs:Sb buffer layers on (111) and (100) fianite substrates were developed to decrease the surface roughness of the PHEMT heterostructure. The buffer layers had a uniform mirror-smooth surface with about 5 nm roughness. Application of the developed buffers made it possible to obtain an AlGaAs/InGaAs/GaAs heterostructures with uniform mirror-smooth surface on fianite substrates and to decrease its roughness by a factor of 10 (to 25 nm). As a result, sufficiently

homogeneous AlGaAs/InGaAs/GaAs multi-layer heterostructures with smooth slightly bloom surface were grown on (001) fianite substrates of 50 mm diameter. Roughness of the heterostructure surface measured using Talysurf interference microscope (3-dimensional topography) was 0.25 μm . This structure was grown using «AIXTRON» installation on (100) fianite ellipsoidal substrate of 2 inch major diameter. The surface of multilayer structure is rather uniform but its roughness reaches the value of 25 nm.

n ⁺ GaAs:Si	$n_{\text{Si}} \sim 6 \times 10^{18} \text{ cm}^{-3}$	40 nm
i-Al _x Ga _{1-x} As	$x \sim 0.24 (>0.23)$	25 nm
i-GaAs		$\sim 0.6 \text{ nm}$
δ -Si	$n_{\text{Si}} \sim 4,5 \times 10^{12} \text{ cm}^{-2}$	
i-GaAs		$\sim 0.6 \text{ nm}$
i-Al _x Ga _{1-x} As	$x \sim 0.24$	4 nm
i-GaAs		1 nm
i-In _y Ga _{1-y} As	$y \sim 0.18 (<0.2)$	11 nm
i-GaAs		30 nm
i-Al _x Ga _{1-x} As	$x \sim 0.24$	50 nm
i-GaAs	$n < 8 \times 10^{14} \text{ cm}^{-3}$	0,5-0,8 μm
CP AlAs/GaAs		(1 nm/ 2 nm) \times 5
GaAs: Sb		100 nm
	Fianite substrate	400 μm

Table 3. PHEMT heterostructure for FET operating in 10-40 GHz range

Structural perfection of AlGaAs/InGaAs/GaAs multi-layer heterostructures on fianite was investigated by means of XRD. DRON-4 device (Ge(004) monochromator, CuK α 1 radiation) was used. $\Theta/2\Theta$ - spectra were recorded at symmetric reflection mode by scanning with 0.1 steps of texture maxima rocking. X-ray diffraction $\Theta/2\Theta$ - spectrum of GaAs (001) / fianite (001) is shown in Fig. 12. The peaks of (Zr,Y)O₂ (004), $2\theta = 73.4$ substrate and of GaAs(004), $2\theta = 66.05^\circ$ buffer layer were recorded. The width of the layer rocking curve $\text{FWHM}_\omega = 1$ that is the evidence of a mosaic structure of GaAs layer. The grain-boundary angle was $\sim 1^\circ$ (Fig. 12a). Preliminary conditions of the growth of AlGaAs/InGaAs/GaAs heterostructures on fianite has shown that the use of (111) fianite substrate with GaAs:Sb buffer layer allowed reaching of mirror-flat homogeneous surface and 10-fold decrease of its roughness up to 0.025 μm value.

Layer-by-layer SIMS analysis of the heterostructures on fianite was carried out using «Shipovnik 3» and «TOF SIMS-5» devices. These devices provide detailed information on elemental and molecular composition in thin sub-surface layers, as well as 3-dimensional analysis. Sputtering was carried out by Cs⁺, 2 keV, raster 250 \times 250 μm , negative ion detection mode, the probe beam Bi⁺, 25 keV, depth resolution $\text{DZ} > 7 \text{ nm}$. The analysis of the AlGaAs/InGaAs/GaAs heterostructures obtained on fianite (Fig. 12b) has shown that its inner topology was in conformity with the assigned scheme (Tab. 3) of the PHEMT-structure.

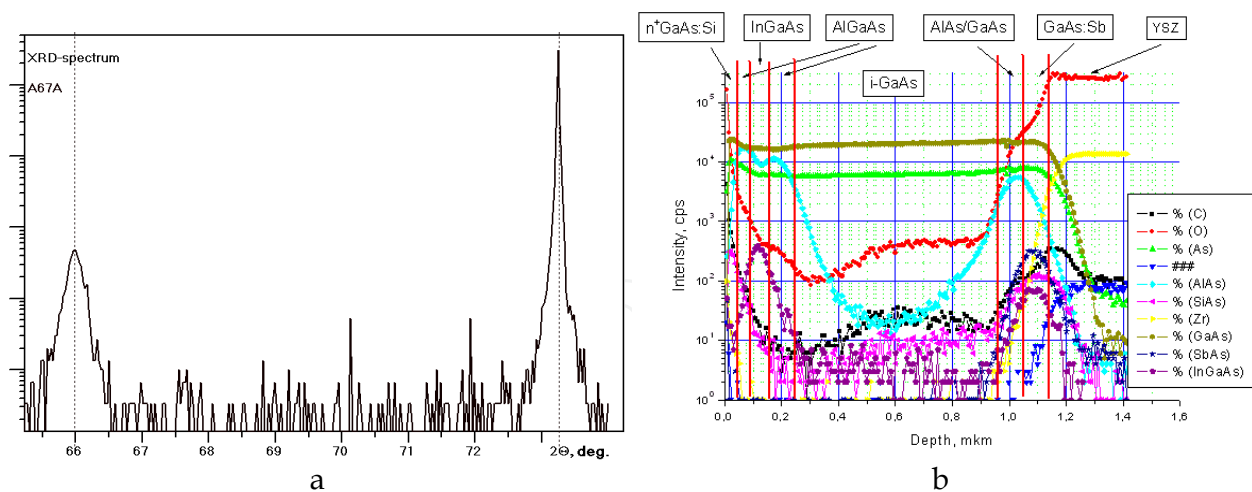


Fig. 12. X-ray diffraction pattern (a) and layer-by-layer secondary ion mass-spectrometry (b) of the multilayer heterostructure AlGaAs/InGaAs/ GaAs (001) / fianite (001).

3.4 A^{III}N films on fianite substrates and buffer layers

Principal difficulty of growth of perfect heteroepitaxial GaN layers is an absence of suitable substrates having good matching with the heteroepitaxial layer. Currently, for the growth of GaN layers Al_2O_3 , ZnO, MgO, SiC, Si, GaAs substrates are in use. Usually, a material with wurtzite structure is grown on a hexagonal substrate, whereas sphalerite - on a cubic one. Fianite as a substrate material for cubic InGaN epitaxy has a number of advantages, such as favorite crystallochemical parameters and high chemical stability. Besides fianite, Si and GaAs substrates with fianite buffer layer were developed in scope of the work. Synthesis of the layer was carried out by laser deposition technique. The growth of fianite films on silicon substrates was conducted with the purpose to evaluate prospects of the use of less expensive large silicon substrates with fianite sublayer instead of monolithic fianite because maximum dimensions of the silicon-on-fianite structures are limited by size and quality of fianite crystals and the corresponding substrates (currently ~50 mm). Another purpose of the study was determination of suitability of fianite not only as a substrate material but also as a gate dielectric. Producing of such substrates will allow integrating GaN-based optoelectronics with a well-developed silicon electronics and gallium arsenide electronics and optoelectronics.

3.4.1 GaN films on fianite substrates

Growth of the films on (111) and (100) oriented fianite substrates was carried out using nucleus layers. 3 types of the nucleus layers were used:

1. Low-temperature GaN nucleus layer with annealing in hydrogen-ammonia atmosphere;
2. Low-temperature AlN nucleus layer with annealing in hydrogen-ammonia atmosphere;
3. High-temperature AlN nucleus layer.

At the use of all of the types of the nucleus layers fianite substrates were annealed in pure hydrogen at ~1070°C before deposition of the nucleus layers.

Hydrogen is conventional carrier gas in MOCVD of III-V materials because it is rather readily can be purified. Similarly, in MOCVD of nitrides of III group hydrogen for the first time was used as a carrier gas. However, later it was demonstrated that in contrast to classic III-V semiconductors, GaN and InN are unstable under hydrogen atmosphere and undergo destruction (etching) at the temperatures used for growth of these crystals. This is an evidence that hydrogen as a carrier gas at the epitaxy of nitrides of III group elements actively participates in the process occurring on the surface of growing layer, in contrast to GaAs. Therefore, in most cases for growth of nitrides of III group by MOCVD ammonia is used as nitrogen source and supplied into reactor in large quantities. For a long time ammonium was because that it inhibits the destruction of a growing film and makes the effect of hydrogen negligible. However, it appears that it is far from the case and hydrogen significantly influenced on the process of the nitrides growth.

The studies have shown that at annealing of LT-GaN nucleus layer, the latter undergo etching in H_2-NH_3 flow hindering growth of a high-quality GaN layer. Application of the low-temperature AlN nucleus layer with annealing in hydrogen-ammonia atmosphere, as well as the high-temperature AlN nucleus layer on (111) and (100) oriented fianite substrates resulted in formation of hexagonal GaN layers comprising a textured polycrystal of hexagonal modification. Scattering angles of the texture for the GaN layers grown on the (111) and (100) oriented substrates were 10° and 15° , respectively.

It has been shown that the high-temperature annealing of LT-GaN buffer layer at 1000-1100C promotes improvement of structural perfection GaN heteroepitaxial layer. The GaN layers on fianite substrates exhibited an intense photoluminescence with maximum at 365 nm.

The conditions of growth of single-crystal GaN layers on (111) and (100) fianite substrates by MOCVD without buffer layer at $850^\circ C$ substrate temperature has been determined. The spectra of $\theta/2\theta$ scanning were obtained with monochromator Ge(400) (fig. 13).

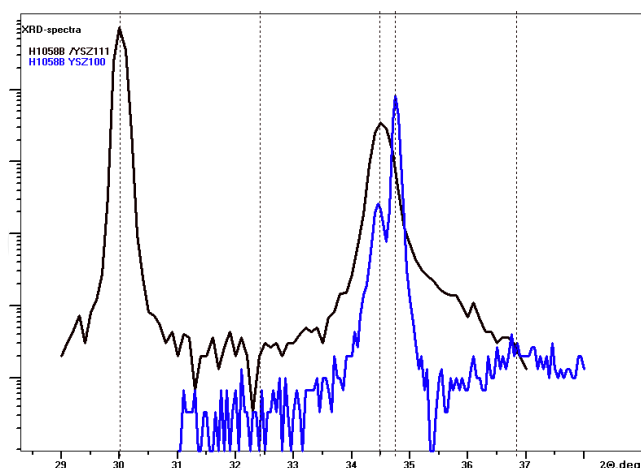


Fig. 13. XRD spectra of GaN on (111) and (100) fianite substrate.

Two peaks of the substrate were observed at 30° YSZ(111) and 34.8° YSZ(200). The layer provides a single GaN(0002) peak at 34.5° . Since GaN (0002) peak is close to YSZ(200) a narrow slit in front of the detector was inserted with the purpose to increase the resolution. GaN_{hex} (0001) was detected on the both substrates at $FWHM_\omega < 1^\circ$ that corresponds to

epitaxial growth. Traces of the polycrystalline phase at 32.4° (suggested 0.1-1.0 intensity units) were not detected.

3.4.2 AlN films on fianite substrates

The AlN films on fianite substrates were grown using MOCPE technique. The $\text{Al}_x\text{Ga}_{1-x}\text{N}$ direct gap semiconductors are very useful in the development of UV photodetectors. By altering Al content in GaN-based solid solutions, it is possible to obtain the material with a forbidden band ranging in 3.43-6.2 eV thus covering 200-365 nm spectral band. This spectral band is of practical importance in UV astronomy, ozone layer monitoring, combustion and water sensors. These films are both of original interest, as well as are useful as nucleating and buffer layers in GaN epitaxy.

Growth of the films was started from thin 20-50 nm nucleating layer. Two growth modes were used: at 650 C with subsequent annealing in ammonia-hydrogen media at 1100 C during 30 min followed by growing-up of the basic layer and high-temperature growth of AlN at the same temperature. Before the deposition of AlN films the fianite substrates were annealed in pure hydrogen at $\sim 1070^\circ\text{C}$. Mirror-flat homogeneous AlN films with the roughness not exceeding 0.6 nm (Fig.14) were deposited on (100) and (111) fianite substrates.

Layer-by-layer analysis of AlN nucleating layer on the fianite substrates was carried out by SIMS using TOF SIMS-5 device (sputtering by Cs^+ , 2 keV, 250×250 raster, negative recording mode, Bi^+ probe beam 25 keV).

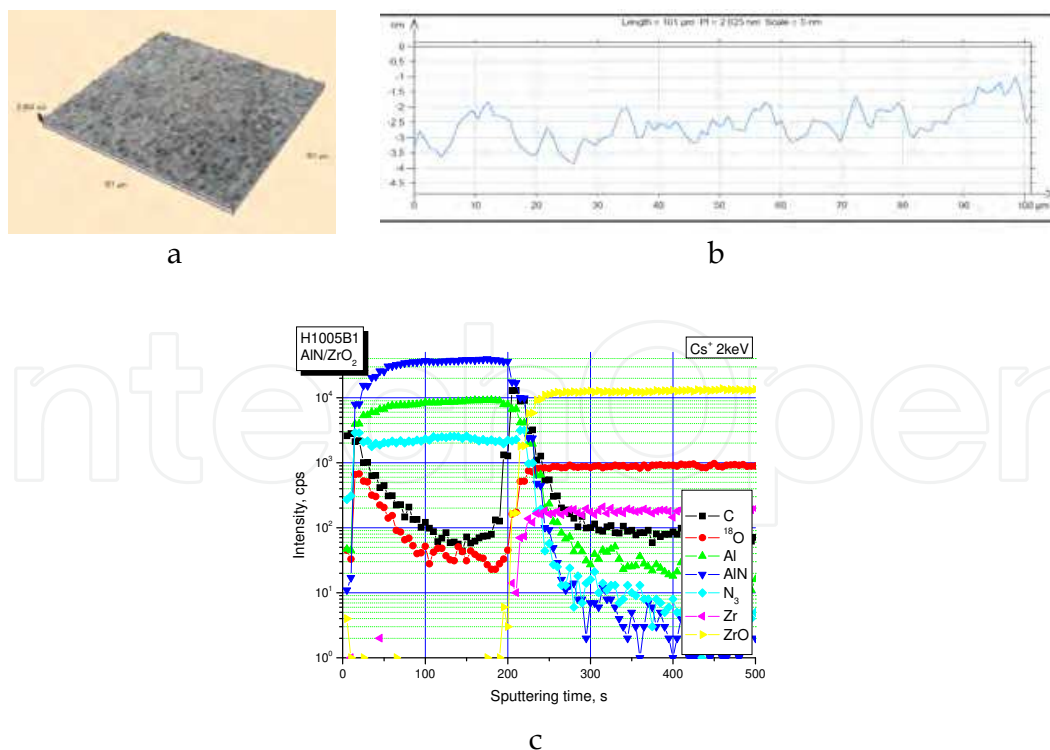


Fig. 14. Interference microscope image (Interference microscope "Talysurf") of surface (a) and surface relief (b); and layer-by-layer secondary ion mass-spectrometry (c) of low temperature AlN seeding layer on fianite substrate.

The study has shown that the layers had uniform distribution of its constituents, the concentration profile of Zr atoms at the hetero-interface being very sharp (Fig. 14c). The use of AlN nucleating layers on the fianite buffering layers allows deposition of continuous and homogeneous GaN layers of hexagonal modification.

3.4.3 Electrically active defects in GaN films on GaAs substrates with fianite buffer layers

Comparative study of density and electric activity of structural defects in the GaN epitaxial films grown on GaAs substrates with various buffer layers were carried out by **Induced bias technique**. Induced bias (IBT) technique has been developed rather recently [30,31]. It is contact-free similarity of induced current technique (EBIC-mode). IBT is nondestructive contact-free diagnostic technique of semiconducting materials and microelectronic devices. IBT is based on detecting of voltage (or charge) generated by an electron probe of scanning electron microscope (SEM). Draft-scheme is shown in Fig. 15 a.

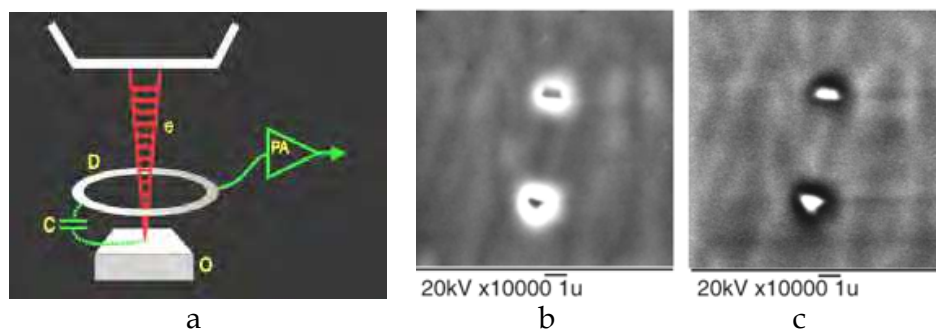


Fig. 15. Outline of induced potential method (a) and scanning electron microscope images of electrically active polygonal defects in GaAs films: secondary-electron emission mode (b); b - induced potential mode (c).

The electron probe (e) scans the surface of a crystal under the study (O). Metal ring (D), in which surface charge generated by electrons through capacitive coupling is induced, is a detector of the signal. The signal from the ring electrode is monitored in the SEM display (or by other measurement equipment) through charge-sensitive amplifier (PA) (Fig. 15 a). The technique allows qualitative monitoring of semiconductor plates, structures and devices identifying electric active inhomogeneities such as dislocations, stacking faults, microfractures, extent of doping by various dopants, all *p-n* junctions and Schottky barriers, etc (see for example Fig. 15 b,c). Quantitative measurements of local fundamental characteristics of semiconductors are also possible (diffusion distance, nonequilibrium carrier lifetime, its surface recombination rate, diffusion barrier height).

The studies have shown that the use of GaAs substrates with porous GaAs layer resulted in a decrease of the electric activity of structural defects in the GaN films and in an increase of its electrical uniformity as compared to GaN films grown on monolithic GaAs substrates. The use of GaAs substrates with double buffer layer (fianite on porous GaAs) allows additionally decreasing concentration of the electrically active defects in the GaN films to more than an order of magnitude (Fig. 16).

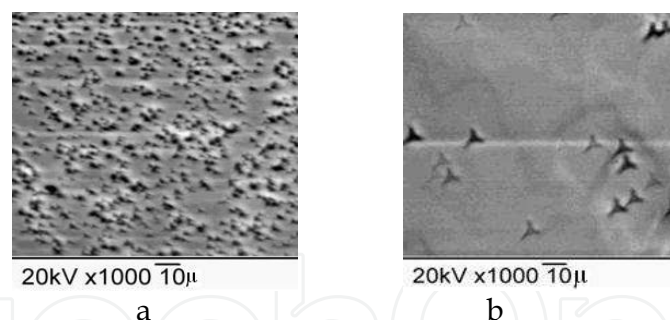


Fig. 16. Electrically active defects in GaN film on GaAs substrate with buffer layers: a – single buffer (fianite); b – double buffer (fianite on porous GaAs).

3.4.4 GaN films on Si and GaAs substrates with fianite buffer layers

Silicon and gallium arsenide are promising substrates for GaN and other $A^{III}N$ epitaxy due to its high quality, large dimensions and a low net-cost, as well as possibility to integrate GaN-based devices with high-developed silicon and gallium arsenide electronics and optoelectronics. However, there are three considerable problems occurring at GaN epitaxy: first, a significant parameter mismatch of GaN layer and Si or GaAs substrates, second, difference of thermal expansion coefficients of the layer and substrates and third, insufficient chemical and thermal stability of the substrates at the epitaxy temperature. Application of various buffer layers, in particular, fianite-based, can be an efficient method for solution of the above problems.

GaN epitaxial films were grown by MOCPE technique using capillary epitaxy on Si and GaAs substrates with various buffer layers. Tri-methylgallium (TMG), arsine (AsH_3) and ammonia (NH_3) were used as Ga, As and N sources, respectively. **Single** (fianite, layer of porous Si or GaAs material) and **double** (fianite on porous Si and GaAs) were tested. The first “prominent” porous buffer layer was suggested to allow decreasing thermoelastic strains in the second heteroepitaxial buffer thus improving its morphology and structure. The upper buffer layer, being chemically stable in the growth medium, provides fine matching with the working heteroepitaxial layer.

The epitaxial structures grown were studied using various techniques: photoluminescence (PL), scanning electron microscopy under induced current (IC) and induced bias conditions and secondary-ion mass spectroscopy (SIMS).

It was established that the use of fianite buffer layer on Si substrate prevents formation of amorphous silicon nitride. The GaN films grown on Si substrates with fianite buffer layer were of hexagonal modification (α -GaN) and had mosaic single crystal structure. It was established that the use of porous Si in the complex fianite/Si buffer allows improving of adhesion of GaN layer and its uniformity by phase composition and thickness.

Layerwise SIMS analysis of the GaN films grown on Si and GaAs substrates with fianite buffer layers has shown that the fianite layer serve as a barrier for diffusion of silicon and arsenium into GaN film from Si and GaAs substrates, respectively (Fig. 17). Good insulating properties of ZrO_2 in double buffer give some possibility to use the technology “Semiconductor on dielectric” which is promising to improve the integration level.

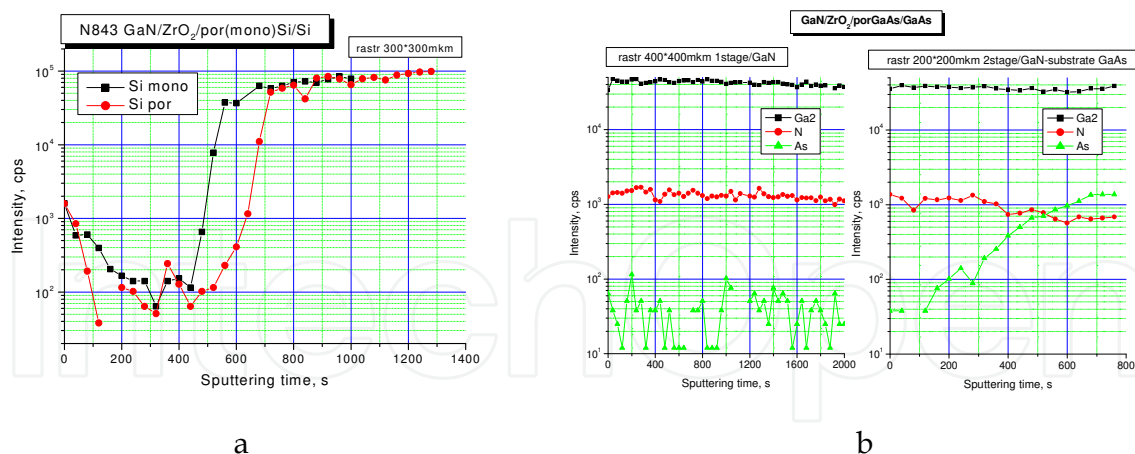


Fig. 17. Layer-by-layer secondary ion mass-spectrometry of GaN/fianite/por(mono)Si/Si (a) and GaN/fianite/porGaAs/GaAs (b) structures.

Comparative studies of PL spectra recorded at 300°K of GaN films grown on a monolithic GaAs substrate and GaAs substrates with various kinds of buffer layers have been carried out (Fig. 18): 1 - single buffer "porous GaAs"; 2 - double buffer "fianite on porous GaAs"

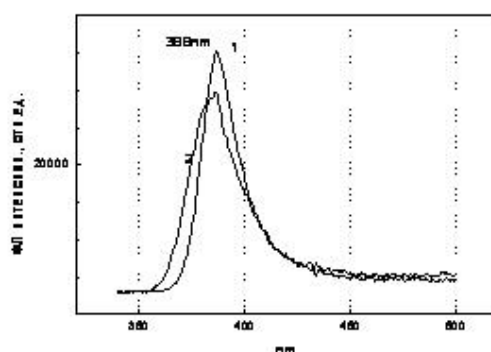


Fig. 18. Photoluminescence spectra of GaN films (300°K) on GaAs substrate with buffer layers: porous GaAs) (1) and double buffer –fianite on porous GaAs (2).

The position of PL peaks in the spectra corresponded to characteristic peak of cubic GaN. Consequently, the use of the single buffer layer of porous GaAs, as well as double buffer layer (fianite on porous GaAs) allows growing GaN films of cubic modification. The growth of GaN film grown on monolithic GaAs substrate in contrast resulted to formation of hexagonal modification.

4. Functional fianite films on Si, Ge and GaAs substrates

4.1 Techniques for deposition of fianite films on Si and GaAs substrates

In recent years a considerable attention was drawn to fianite films on silicon due to its electric and optic device applications, such as isolating layers in SOI (silicon-on-insulator) devices [32], gate dielectric in Si- [33, 34], SiGe- [35] and A^{III}B^V-based [36] device structures, buffer layers for producing of optic coatings of films of various semiconductors [37–40], superconductors [41–43], ferroelectrics, etc.

Various techniques can be used for the producing of fianite films on silicon and other semiconductors, including magnetron [39, 40, 44-46], laser and electron-beam [47-49] sputtering, molecular-beam epitaxy (MBE), as well as gas-phase chemical deposition [50]. The choice of a specific technique is determined by further designation of a fianite film, possibility to produce the film of maximum structural perfection, as well as technologic potentialities of a technique. So, MBE technique is more suitable for deposition of the thinnest fianite film for the use as a gate dielectric. Magnetron and laser sputtering are more favorable for fianite layers used as buffer layers with subsequent growing semiconductor films, including $A^{III}B^V$ compounds. In [39] fianite films were deposited on Si and GaAs substrates using magnetron, laser and electron-beam sputtering techniques. The films obtained by magnetron sputtering were of the best structural perfection [39].

4.2 Growing of fianite layers on silicon and gallium arsenide

The growth of fianite films on silicon and gallium arsenide substrates was carried out with the purpose to evaluate the prospects of using less expensive and more large Si and GaAs substrates with fianite sublayer instead of monolithic fianite substrates because, currently, maximum size of the latter is ~50 mm. Another purpose was determination of an opportunity to use fianite not only as a substrate but also as insulating layers material alternative to SiO_2 , SiC, Si_3N_4 , protecting and insulating layers, as well as a gate dielectric for multi-layer "semiconductor-dielectric" structures. Producing of such substrates will allow integrating GaN-based optoelectronics with a well-developed silicon electronics and gallium arsenide electronics and optoelectronics. Magnetron and laser sputtering were used for deposition of fianite films on silicon and gallium arsenide fianite films on porous Si and GaAs.

With the purpose to improve quality of fianite films and its adhesion to Si and GaAs substrates opportunities of the use of porous layers of the material were studied.

The following results were obtained:

- appropriate regimes of deposition of porous GaAs layer on GaAs (111) substrates of n- and p-conductivity types were developed;
- appropriate regimes of deposition of the uniform mirror-flat fianite layer on GaAs (111) substrates of 18x18 mm size were established;
- it has been demonstrated that the use of the porous layers allowed an improvement of adhesion of fianite with GaAs layers;
- the samples of fianite/GaAs, fianite/Si epitaxial substrates have been obtained for subsequent growth of $A^{III}N$ films.

High mechanical and chemical stability of fianite and absence of pores confirmed the prospects of its application as protective and stabilizing coatings substrates.

4.2.1 Magnetron sputtering technique

Magnetron systems are related to diode-type sputtering systems. The sputtering occurred due to bombardment of a target surface by gas ions (usually Ar) forming in plasma of anomalous glow discharge. A material ions knocked out the target subjected to the bombardment are captured by magnetic field and maintained complex cycloidal movement by closed trajectory in vicinity of the target surface. High sputtering rate, which is a feature

of magnetron systems, is achieved by an increase of the ion current density due to localization of plasma by means of high transverse magnetic field. The increase of sputtering at simultaneous decrease actuation gas pressure allows a significant decreasing contamination of the films by alien gas impurities. Fianite was grown up on Si and GaAs substrates using unbalanced magnetron system. Fianite crystals were used as a target. Si substrate subjected to the sputtering was heated by IR radiance. Preparation of the substrates included degreasing, removing of the oxide and passivating of the surface in ammonium-peroxide solution. Optimization of the conditions of the growth of fianite films on Si substrates was carried out by varying of the sputtering rate, temperature of the substrate and residual gas pressure.

Bombardment of the target leads to dissociation of zirconium and yttrium oxides to ZrO, Zr, YO, Y, O₂. That is why such parameters as sputtering rate and residual gas pressure considerably influence on stoichiometry of the resulting film. Energy of the evaporating particles is rather low (~0.5-10 eV), so for the epitaxial growth of fianite film a high temperature of Si substrate and optimal rate of the condensate supply are necessary.

4.2.2 Laser sputtering technique

Experimental installation for deposition of fianite films was a sputtering system composed by vacuum device and eximer laser. The system has been designed and manufactured in IPM RAS.

Operational oxygen pressure was maintained by vacuum system supplied with a mechanical pump and CHA-2 letting system. Evaporation of the target was performed by LPX200 eximer laser radiation working on KrF mixture. Wavelength of the radiation was 248 nm, pulse duration 27 ns, the pulse energy 350 MJ (pulse power 1.3×10^7 W), repetition frequency 50 Hz. Optical system providing a focusing of the laser beam on the target surface consisted of quartz prisms and 30 cm focal distance lens. The laser beam spot on the target surface was 1×4 mm². The energy density on the target surface was ~10 J/cm². The distance between the target and substrate was 60 mm. Cylindrical targets of 15-20 mm diameter and 10-30 mm length were used in the installation. In order to prevent local overheating of a target and to provide uniform material drift rotation and axial movement of the target was used. Possibility of conducting pre- and post-growth annealing under oxygen atmosphere at 10 Pa - 100 kPa pressure and at up to 750°C temperature is a peculiarity of the installation.

Ceramic target of $(\text{ZrO}_2)_{1-x}(\text{Y}_2\text{O}_3)_x$ with $x=0.1$ composition was used for deposition of fianite films. The deposition was carried out on Si and GaAs substrates heated to 600-800°C temperature under oxygen atmosphere at approximately 10 Pa. The growth rate of YSZ films was about 0.02 nm per pulse. Contactless heater of substrates (heating by irradiance) was an original peculiarity of the sputtering system. The heater comprises vertically positioned quartz tube (of 30 mm inner diameter) supplied with refractory stainless steel heating coil on its outer surface with up to 1 kW power of the heater. Monitoring and maintenance of the assigned temperature (with $\pm 5^\circ\text{C}$ precision) were carried out using precise regulating device and Pt-Rh thermocouple positioned under the heating coil. A substrate was fitted in a holder and positioned inside of the quartz tube. Loading of substrates and oxygen supply was maintained through the upper end of the tube.

Technology of growth of dielectric fianite films using the laser sputtering consists of the following stages:

1. A substrate is loaded to the sputtering system and vacuum chamber is evacuated up to ~ 1 Pa residual pressure.
2. Letting-to-oxygen is done up to the pressure required.
3. Rotational movement drive of the target is switched on.
4. A substrate is heated up to deposition temperature.
5. The eximer laser (the pulse energy 350 MJ, repetition frequency 50 Hz) is switched on and the sputtering is started.
6. Followed by the achievement of assigned thickness of the film the laser is switched off.
7. Followed by the end of the film growth the chamber is filled with oxygen up to the pressure required.
8. The structure is annealed.

The substrate heater is switched off and the substrate is cooled to room temperature.

4.2.3 Initial stages of deposition and structure of fianite buffer layers on Si and GaAs substrates

The application of fianite as a buffer layer will allow a solution route to another very important problem – epitaxy of $A^{III}N$ compounds on Si and GaAs substrates having large dimensions, high quality and low net cost.

Single crystalline heteroepitaxial fianite layers of 1000 Å thickness were grown on silicon substrates of up to 50 mm diameter in vacuum chamber at $p \sim 2 \cdot 10^2$ Pa pressure, sputtering rate $V_s \sim 60$ Å/min and substrate temperature $T_s \sim 800^\circ\text{C}$.

The studies have shown that the layer became continuous as from 100 Å thickness.

X-ray structural studies of $ZrO_2\text{-}Y_2O_3/\text{Si}$ structures have shown that the fianite film is single phased and consisted of two layers with different rocking curve values: $0,20^\circ$ for the upper layer and $0,96^\circ$ for the lower one. Epitaxial relation between the film and the substrate was $(100) [100]\text{Si} // (100)[100]ZrO_2\text{-}Y_2O_3$. The relation was established using diffraction measurements under following regimes: $\Theta/2\Theta$ scanning (simultaneous rotation of the detector and sample over goniometer axis) and Ψ - scanning (rotation of the plate in a proper plane at fixed detector position). The former regime was used to determine orientation of the composition plane, the latter – mutual orientation of unit cells of the film and the substrate in the composition plane.

Spectra of the Ψ - scanning of $(ZrO_2\text{-}Y_2O_3)/\text{Si}$ structure for the asymmetric (422) reflection of the film (b) and the substrate (a) are shown in Fig. 19.

The absence of additional peaks and high peak maximum-to-background ratio ($\sim 10^3$) are the evidence for $ZrO_2\text{-}Y_2O_3$ layer is a perfect single crystal film. The fianite buffer layers grown on Si and GaAs were used for $A^{III}N$ compounds epitaxy.

4.2.4 Some difficulties in deposition of the fianite layers on silicon

Growth of fianite-on-silicon structures of high quality featuring with sharp interfaces is associated with significant difficulties because of a number of principal problems.

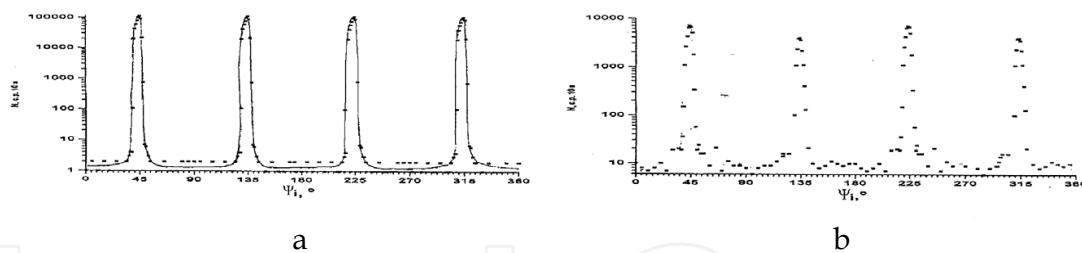


Fig. 19. Ψ scanning spectra for (422)reflection of YSZ substrate (a) and the film (b)

First, silicon surface readily undergoes to transformation into SiO_2 amorphous layer due to either interaction with oxygen-containing fianite film, or oxidative atmosphere usually used at the fianite growth. As it has been shown by calculations, fianite should not react with silicon substrate to form SiO_2 , which has low dielectric constant value, at a direct contact [51]. However, in practice, it is very difficult to avoid formation of this layer at the fianite deposition or subsequent high-thermal treatment [52,53]. Therefore, a development of special technological tools is necessary. One of the routes to solve the problem has been suggested by the authors [54]. Thin Zr or Y layer was deposited on Si substrate before fianite deposition. The metals absorb oxygen from SiO_2 layer because free energy of both fianite and Y_2O_3 formation is lower than of SiO_2 one [55]. That leads to a decrease of the layer thickness.

Second, oxygen from the fianite layer readily diffuses to a silicon substrate or reacts with silicon surface. Secondary phases occurring as a result of the reaction disturb silicon crystal lattice and hinder a perfect growth. Under these circumstances, the fianite layers on Si substrates are of amorphous or polycrystalline structure. At the development of gate dielectric technology these issues are of peculiar importance because thickness of the last layer is about some nanometers.

Therefore, the above data show that the problem of deposition of fianite layers on Si substrates is of great interest. The problem of improvement of quality of the layers seems to be very urgent because of a number of principal difficulties occurring due to peculiarities of physic-chemical properties of the materials considered resulting in reactions at the growth and subsequent thermal treatment stages. The synthesis of perfect fianite layers on Si requires a development of special methods to decrease the influence of amorphous SiO_2 layer at the substrate-layer interface.

4.3 Development of the techniques of fianite films etching

To choose the most appropriate method and conditions of fianite film etching, we have tried out the main methods of etching used in microelectronics technologies: liquid (wet), plasmachemical, and ion-beam methods of etching.

4.3.1 Liquid etching

For fianite film liquid etching (by analogy with ZrO_2) the following etchants were used:

- etchant $\text{HCl}:\text{HF}:\text{H}_2\text{O}$ (10:1:5). Fianite films were found to be resistant to this etchant;
- strong acids: H_2SO_4 , HF, HCl, HNO_3 ;
- aqua-regia: $\text{HNO}_3:\text{HCl}$ (3:1).

The film was found to be chemically resistant to all of the above listed reagents. So we tried out all the most chemically active reagents that traditionally are used for dielectric film liquid etching in photosensitive devices production. On the one hand, this evidences resistivity of photosensitive devices with fianite protective layers to corrosive medium exposure. On the other hand, such properties cause technological difficulties. To settle the problem, we have searched for other methods of etching.

4.3.2 Plasmachemical etching

In case of plasmachemical etching, a mask of 1.3 μm thick FP91-20-1 photoresist hardened at 120°C during 20 minutes was used. A diode type plant was used. The discharge power was between 200 and 350 Wt, discharge frequency was 105 KHz. Temperature inside the reaction chamber was varied from 20°C to 90°C, etching time - from 10 to 35 minutes. Mixtures of $\text{CCL}_2\text{F}_2+\text{Ar}$, $\text{CCL}_2\text{F}_2+\text{He}$, and $\text{CCL}_2\text{F}_2+\text{O}_2$ of various percentages were used as reagent gases. The pressure in the processing chamber during samples etching varied from 0.2 to 0.85 mBar. The samples surface texture after etching depends upon the etchant, the process conditions, and the preliminary surface treatment. Prior to etching, the samples were treated with Ar and He ions. Loose texture surface was observed on the samples; such texture had been formed probably by precipitation of products of reaction on the sample surface. Water vapor and oxygen may be absorbed on the reactor surface and slow down etching till they completely react with the working gas. The period of etching slow down may be decreased by eliminating of the said factors with the help of a "loading lock". For this purpose, another construction of the plant was chosen that applied the reactive-ion technology of film etching with the loading lock. Use of such plant made it possible to combine glow discharge plasma and the chemical medium providing etching. The medium consists of charged particles, radicals and neutral particles participating in chemical reactions on the film surface. Volatile products are formed in the medium. Positive ions being accelerated in the interelectrode space bombard the surface of plates thus finishing material removing.

The following conditions of the process of fianite film etching were examined:

Working pressure in the reactor	0.03-0.08 mBar
Discharge power	320-800 Wt
Discharge frequency	13.56 MHz
Etching time	10-45 minutes

Adding of O_2 to chloride bearing plasma increases concentration of Cl and suppresses polymer film forming on the sample surface. Adding of inert gases stabilizes plasma. Stabilization may be achieved due to thermal properties of the discharge gas used, especially in case of helium adding.

Unfortunately, in this method the rate of film etching was found to be low; besides, the problem of mask selection occurred. That is why, the studied technologies of plasmachemical and reactive-ion etching for fianite films are rather inefficient. But they may be used for gold contacts etching.

Of cause, capabilities of the investigated technologies may be expanded by use of more active reagents, such as CCl_4BC_3 . But, such reagents are referred to extremely hazardous

substances. Any work with such substances requires availability of specific production or laboratory premises, equipping of which is allowed only in specific industrial areas and causes additional labour and financial costs. That is why further researches were devoted to fianite film etching using ion-beam method.

4.3.3 Ion-beam etching

This method is based on material scattering under ion bombardment. The sample (fianite-semiconductor structure) was fixed on a holder. The holder was cooled to avoid overheating. Ions were generated in a direct current discharge in a separate "ion" gun, were focused and accelerated towards the samples treated.

A fianite film of 1000 Å was etched through a photoresist mask with the help of ion-beam etching during 35 minutes.

4.4 Characterization of the fianite films

The fianite films were studied by means of scanning electron microscopy, ellipsometry and CV-parameters measurement techniques. The films parameters were found as follows:

- optic refractive index $n_{\text{ок}} \sim 2,1 \div 2,2$;
- dielectric constant $\varepsilon \sim 25$;
- absence of defects of porosity type (in 30 mm diameter sample).

4.4.1 The capacity-voltage characteristic measurements of fianite-on-silicon" structures

The capacity-voltage (CV) characteristics of the structures supplied with fianite films deposited on *p*-Si and *n*-Si substrates were measured.

Capacity measurements provide evaluation of dielectric properties of the films under the study: dielectric constant ε and dielectric loss $tg\delta$. The application of multifrequency device allows determination of frequency dependencies of dielectric constant and high-frequency loss in dielectric films. Since the dielectric film is deposited on semiconductor a MIS structure (metal-insulator-semiconductor) is formed, so the CV-measurement provides additional information concerning the semiconductor and the dielectric-semiconductor interface, namely, type of the semiconductor conductivity (n- or p) and concentration of the dopant, flat band barrier voltage V_{fb} , density of boundary states and a charge induced in the dielectric.

The device used for CV- measurements allowed determining of capacity and high-frequency conductivity of the structures, as well as its dependency on the applied voltage. The measurements were carried out at 500 KHz and 1 MHz frequencies. Direct potential bias range was ± 40 V. Thermally sputtered Al of 1 mm surface diameter was used as the contacts. The results obtained are shown in Fig. 20.

"Al-fianite-Si" MIS structure parameters: flat band barrier voltage - 4 V for 180 nm film and 1.5 V for 20 nm film; density of boundary state charge $\sim +10^{12}$ cm⁻².

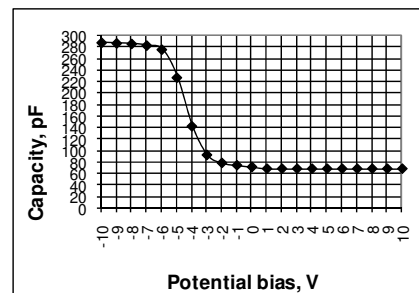


Fig. 20. CV- characteristics of fianite-on- *p*-Si sample

4.4.2 Investigation of ZrO₂ films on Si and Ge substrates by means of scanning electron microscopy

The ZrO₂ films were studied using scanning electron microscopy. All of the films studied were porous-free. Since square of the samples studied was 5-6 cm², it is possible to consider the porosity value at least not exceeding 0.15-0.2 cm². For comparison, it is worth to mention that porosity of SiO₂ films is 4-8 cm². Therefore, it is possible to consider ZrO₂ films as the protective layer for Ge devices actually superior SiO₂ films because its porosity decreased in 1.5-2 orders of magnitude.

The study of morphology of the films deposited by magnetron sputtering technique at high magnification has shown its satisfactory homogeneity. Some regions of the surface featured by a relief composed by quasi-spherical hills of 500-600 nm in diameter and exhibiting lateral periodicity. Analytical study of the films has shown an absence of inclusions of impurities.

An attempt to study mechanism of formation of the films with the purpose to optimize conditions of magnetron sputtering was done using electron microscopy (JSM JEOL 5910 LV). The particles were identified by means of electron probe. The film was removed by polishing using diamond paste with 2.5-4 μm particle size. This abrasive size was chosen to minimize decreasing particle size of the film constituents at the polishing. The obtained material was flushed by ethanol (9-12 purity grades "for microelectronics") and the suspension was put in plastic syringes (1 ml). In order to disintegrate aggregates ultrasonic (US) treatment was carried out. The US dispersion was conducted using «Sapphire 3M-1.3» US device with 35 GHz operational frequency. The syringes were inserted to the device chamber filled with water. The chamber was thermostated at 27°C. Followed by 3 min of the US treatment the suspension was aspirated onto conductive (graphitized) ribbon for subsequent microscopy study. The study has shown that the largest constituents of the zirconia film were quasi-spherical particles of 50-100 nm size that explained X-ray amorphous nature of the film. It is possible to suggest that formation of larger elements of the relief occurred by enlargement of such particles. The reasons of local enlargement (formation of spherical hills) can be gradients of temperature and mass-transfer, as well as occurrence of impurities. The observations allowed refining the refine conditions of the sputtering of ZrO₂ and fianite films in order to minimize surface roughness.

4.5 Fianite as a gate dielectric

Recently, a sharp surge of interest in the use of fianite as a gate dielectric in CMOS technology has been observed. It is associated with an increase of leakage current at the use

of conventional SiO₂ by increasing of integration level. That requires a change of SiO₂ over dielectrics with higher dielectric constant (high-k materials) [33-35,51]. The recent studies have limited possible alternatives to fianite, HfO₂, ZrO₂ and its silicates. For example, ZrO₂ has high dielectric constant value, good dielectric properties (5.8 eV energy gap width) and rather good crystallochemical matching with Si [56] (see Fig. 5). Intel Corp. – one of the leaders of the world electronics, has demonstrated that the change of SiO₂ over HfO₂ as a gate dielectric in 45 nm technological process allows decreasing leakage currents (which became a serious problem for transistors) by more than two orders of magnitude [57].

Comparison of fianite and SiO₂ films [34] with electrical equivalent oxide thickness of about 1.46 nm has shown that the leakage current for fianite was four orders of magnitude lower than that of conventional SiO₂ gate oxides.

The hysteresis and interface state density in this film was measured to be less than 10 mV and $2.0 \times 10^{11} \text{eV}^{-1} \text{cm}^{-2}$. It demonstrated that crystalline oxide on semiconductor could be used for future generation of semiconductor-based devices.

It is worth to note that quality of the synthesized fianite, as well of the interfaces [85], is very important for integration of such a dielectric to the CMOS technology currently in use.

Synthesizing of fianite-on-silicon structures of high quality featuring with sharp interfaces is associated with significant difficulties because of a number of principal problems.

First, silicon surface readily undergoes to transformation into SiO₂ amorphous layer due to either interaction with oxygen-containing fianite film, or oxidative atmosphere usually used at the fianite growth. In practice, it is very difficult to avoid formation of this layer at the fianite deposition or subsequent high-thermal treatment. Therefore, a development of special technological tools is necessary.

Second, oxygen from the fianite layer readily diffuses to a silicon substrate or reacts with silicon surface resulting in SiO₂ formation having low dielectric constant value. At the development of the gate dielectric technology these issues are of peculiar importance because thickness of the last layer is about some nanometers.

One of the routes to solve this problem is in application of low-temperature growth and annealing regimes, as those, which were used in the series of experiments described below, Type of a substrate and the annealing media were also varied. Conditions of the synthesis of the fianite/Si structures are given in Tab. 4. XRD technique has shown that fianite layers obtained by laser deposition at room temperature were of amorphous structure.

Sample	T of growth, C	Annealing, 600 C, 10 min	Film thickness, nm	Substrate
z 1	room	without annealing	~20	Si
z 2	room	vacuum	~20	Si
z 3	room	oxygen	~20	Si
z 4	room	oxygen	~20	Si <Sb>
z 5	600	oxygen	~20	Si

Table 4. Parameters of growth and annealing of the fianite-on-Si films

Subsequent post-growth recrystallization annealing resulted in arising of a polycrystalline phase in the layer. At the same time, the layers sustained mirror-flat and uniform. Profile of the surface of z4 sample (Table 4) obtained using Talysurf interference microscope is shown in Fig. 22 a. Roughness of this ZrO_2 surface was estimated as $Sq = 0.852$ nm that is not practically differ from roughness of the Si substrate used for the fianite growth ($Sq = 0.7877$ nm).

Preliminary studies of gate properties of thin (10–15 nm) fianite films obtained by laser deposition on Si substrates have been carried out. The studies conducted on the test structures with deposited Al contacts have shown that thin fianite films featured with low values of loss currents, minimum values being 10^{-12} A/cm² at 1V voltage (Fig. 21 b, samples z 3 and z 4).

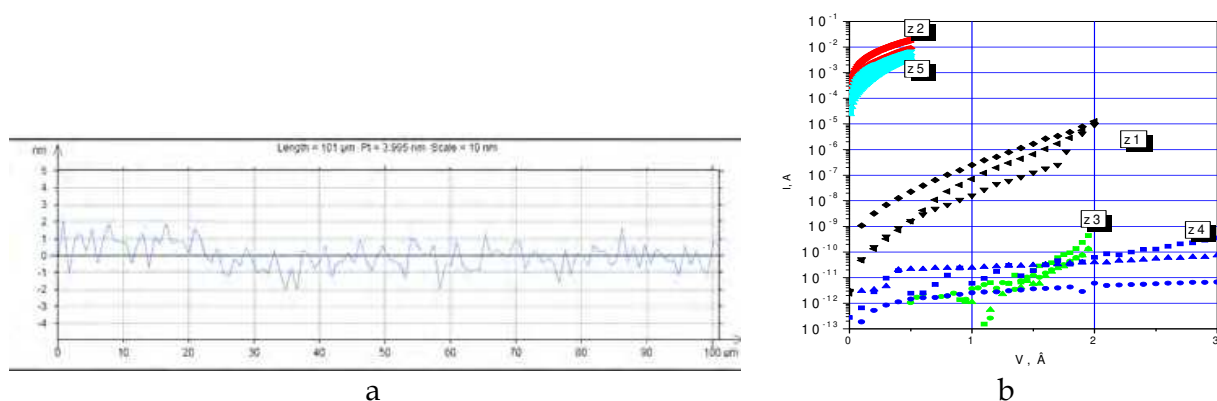


Fig. 21. Surface roughness of fianite film on Si substrate, sample Z4 (a) and leakage current of Al/fianite/Si structure (b), samples z 1 - z 5 were prepared under different conditions.

4.6 Fianite and ZrO_2 as protective and stabilizing layers on Ge and Si substrates and multilayer structures

4.6.1 Deposition modes

For magnetron deposition of fianite and zirconium dioxide films, 2 types of vacuum evaporation Leybold Heraeus units were used with different target dimensions: 70 mm in diameter for fianite and 203 mm – for ZrO_2 (table 5).

HF magnetron and direct voltage sputtering techniques were tested. The latter technique did not provide sufficient film growth rate, that is why magnetron HF sputtering (13.56 MHz) was chosen. The optimal modes of fianite and ZrO_2 sputtering are also shown in table 5.

Target Material	Fianite	ZrO_2
Plant Z	Z-400	Z-550
Target diameter	Ø 70 mm	Ø 203 mm
Argon pressure	$5 \cdot 10^{-3}$ mBar	$5 \cdot 10^{-3}$ mBar
Power	~ 500 Wt	~ 400 Wt
Film growth rate	100 Å/min	~ 50 Å/min

Table 5. Optimal Modes of Fianite and ZrO_2 Sputtering

In case of low magnetron power, plasma is unstable ("blinking plasma"); in case of larger values of discharge power, the growth rate increases, but irregularity of substrate surface layers and growing film coarse-graining are possible. Fianite sputtering requires higher power than in case of ZrO_2 ; provided that the growth rate is twice as much than in case of ZrO_2 .

The developed technique of magnetron sputtering made it possible to vary the fianite film thickness between 600 and 2000 Å. Ge and Si plates with fianite film thereon were made using this technology. Ge samples with fianite film were used to try out further operations of device structures making: photolithography and etching.

4.6.2 Protective and stabilizing properties of fianite films on Ge

Inorganic dielectric coatings are usually used for passivating and protection of p-n transition surface, as shielding and thermal compensation layer at ion implanting and for interference antireflecting protection. Passivation of the surface is the most important issue for manufacturing of germanium photodiodes because natural GeO and GeO_2 oxides are unstable and, so, can not be considered as the only passivating coatings. It is one feature distinguishing Ge and Si devices (the latter have stable and effective coating of its own SiO_2 oxide). This oxide film deposited from a gas phase is of the most frequent use for photodiodes with p+ - n-structure. It has positive charge and by attracting electrons to the surface prevents growth of p-channels thus decreasing probability of generation in the layer. It is worth to note that for improved reliability and stability of characteristics of photodiodes it is necessary to maintain surface state density at $10^{11} \text{ cm}^{-2} \text{ eV}^{-1}$ level. However, this passivating technique is far from ideal because high porosity of SiO_2 films that decreases humidity resistance and reliability of the devices.

In order to improve dielectric properties of the protective coating fianite films deposited by magnetron sputtering were used. The opportunity of its application for maintaining high-quality practically porous-free protective coating has been confirmed earlier by the experiments.

It has been demonstrated that the use of the fianite protective layer in Ge-structures instead of SiO_2 eliminated pulse noise and thus considerably improved photoelectric and performance characteristics of these devices. It has been established that the improvement was related to more uniform nature of the fianite films, in particular, absence of pores, in comparison with SiO_2 films, which containing defects in form of pores.

4.6.3 Some properties of the device structures supplied with zirconium dioxide films

Photoelectric characteristics and noise of germanium photodiodes supplied with ZrO_2 and SiO_2 films described above have been investigated. Monochromatic sensitivity of these photodiodes is typical for germanium devices and equals to 0.5-0.6 A/W (at 1.06 and 1.55 μm wavelengths). The change SiO_2 over ZrO_2 resulted in somewhat decrease of a dark current (on average for 10%). Main improvement of the photodiodes quality achieved due to the application of ZrO_2 films revealed at the noise studies. Under the voltage exceeding operational one (that corresponds to accelerated reliability testing conditions) the check samples with SiO_2 films have shown pulse noise of telegraphic type in the oscillogram, which can be associated with processes of energizing- deenergizing of the surface

conducting channels [59]. The defects occurring because of the presence of pores in SiO₂ films are a probable cause of arising of the channels. In the batch with ZrO₂ protective films only shot noise, which is in principle unavoidable, was observed. More detailed results of the device studies are presented in [60].

Thus, the studies performed on fianite and zirconium dioxide films, as well as on the device structures developed using these films have demonstrated the advantages of zirconia-based solid solutions in application to photosensitive apparatus technology.

4.7 Studies of optical properties of ZrO₂ films

Optical refraction of ZrO₂ equals to 1.98÷2.1, that is close to fianite one, therefore this material is also promising for antireflection coatings. Determination of the refraction constant n and monitoring of the film thickness d were carried out using ellipsometry technique. The experimentally determined values of d depended on duration of the films growth and varied within 600Å - 1100Å range.

The films obtained have shown rather high refraction: ~2÷2.1. These values were significantly higher than that of SiO₂ (1.45).

In theory, considering an incident beam from air (vacuum), it is possible to decrease the reflection to zero when the refraction constant of an antireflecting film corresponds the following equation:

$$n = \sqrt{n_n}$$

where n_n - refraction constant of a semiconductor. In case of Si and GaAs $n_n \sim 3.5\div 4$, thus $\sqrt{n_n} \sim 1.9\div 2$. Therefore, the ZrO₂ films obtained actually satisfy perfect antireflection of Si and GaAs - based devices from the viewpoint of n . Moreover, the difference in n -values of SiO₂ and ZrO₂ films provides an opportunity for the antireflection over a broad spectral range due to application of binary SiO₂+ ZrO₂ antireflecting coatings. The dependency of the reflection constant on wavelength of silicon sample coated with ZrO₂ film of 1200Å thickness is presented in Fig. 22. Theoretical absorption minimum corresponds to $\lambda = 4nd = 4 \cdot 2.1 \cdot 0.12 \approx 1 \mu\text{m}$.

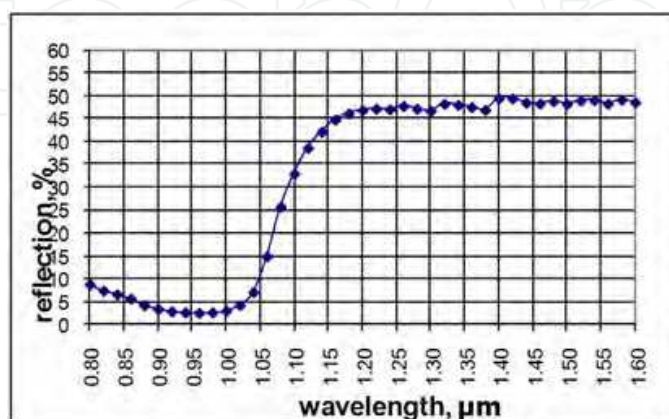


Fig. 22. The dependency of the reflection constant on wavelength of silicon sample coated with ZrO₂ film of 1200Å thickness.

As it is apparent from Fig. 23, the reflection minimum was approached at $\lambda_{\min} = 0.97 \mu\text{m}$. Thus, the experimental results are in conformity with the theory practically complete.

Therefore, the ZrO_2 film ensures high antireflection quality: at λ_{\min} the reflection loss does not exceed 2-3 %. The data obtained confirm that ZrO_2 is an excellent material for antireflecting films, as well as fianite.

5. Silicon and III-V solar cells with fianite antireflecting layer

5.1 Anti-reflection properties of fianite film on Ge and Si

In theory, it is possible to eliminate the reflection completely (at the corresponding thickness of a film d) at $n_d = \sqrt{n_f}$, where n_f – optical refraction constant of a semiconductor. Since for Si and Ge the constants equal to 3.7 and 4, respectively, the reflection is completely eliminated at $n_d = \sqrt{n_f} \approx 2$. Therefore, a dielectric having its optical refraction constant $n_d = \sqrt{n_f} \approx 2$ (at $n = 3.7 \div 4$) can be considered as an optimal material for the antireflecting film for solar cells and the other photosensitive devices. Theoretically, it is the case at the film thickness, which is equal to a quarter of optical wavelength $W = \lambda / 4n_d$, such dielectric allows a complete elimination of the reflection loss ($R=0$).

The refraction constant of SiO_2 ($n = 1.47$) is considerably lower than that value. At this n value it is impossible to maintain the reflection loss lower than 10%. Refraction constants of fianite and ZrO_2 are within (2.15÷2.18) and (2.13÷2.2), respectively, - that is close to the above optimum value. Thus providing an evidence that fianite and ZrO_2 are very promising as antireflecting coatings for solar cells and the other photosensitive devices based on Ge, Si and A^{III}B^V compounds.

Experimental dependencies of antireflection (as dependencies of the reflection on wavelength) of fianite films on Si and Ge have been plotted (Fig. 24).

The plots apparently demonstrate that the reflection drops to 0 – 1.5 % in the minima.

Experimental study of antireflective properties of fianite oxide applied to Ge was performed. By the reason that, germanium photodetectors are designed for detecting radiation generated by lasers with wavelengths $\lambda = 1.06; 1.3; 1.54 \mu\text{m}$, the thickness of the antireflective fianite film was chosen as $W = 1300 \text{ \AA}$; such thickness provides for minimal reflection losses in the said wavelength range $\lambda = 1.06-1.54 \mu\text{m}$. Fig. 23 a shows the comparison of experimental (thin line) and theoretical (bold line) $R(\lambda)$ curves. The theoretical $R(\lambda)$ curve was calculating using the following formula:

$$R = 1 - \frac{4n_{II}n_{OK}^2}{n_{OK}^2(n_{II} + 1)^2 - (n_{II}^2 - n_{OK}^2)(n_{OK}^2 - 1)\sin^2(2\pi n_{OK}W/\lambda)}$$

According to the above formula, reflection may fall practically to zero at the optimal value of n_{OK} (note, that in case of SiO_2 anti-reflective film, for which $n_{OK} = 1.47$, it is impossible to obtain reflection lower than 10%). The minimal reflection is achieved at the following wavelength λ_{\min} :

$$\lambda_{\min} = 4Wn_{OK}$$

As it is shown on Fig. 24a, in the range of fundamental absorption (for $\lambda < 1.65 \mu\text{m}$) the experimental curve 1 coincides with the theoretical curve 2. Some discrepancy at higher wavelengths ($\lambda > 1.65 \mu\text{m}$) appears due to deep penetration of such radiation and its reflection from the back surface. It is important that at the optimal wavelength ($\lambda = 1.12 \mu\text{m}$), fianite film provides for ideal antireflective properties – the reflection is actually absent. In rather large range 0.88 - 1.55 μm , into which radiation wavelengths of most wide spread lasers fall, the losses for reflection do not exceed 10%.

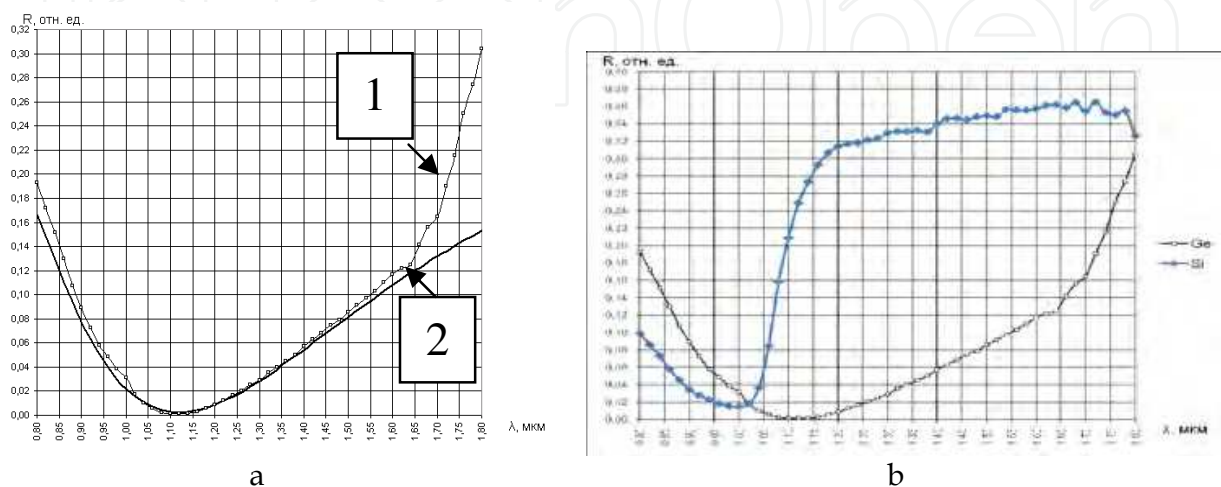


Fig. 23. Experimental (1) and theoretical (2) dependencies of the reflection on wavelength in Ge-fianite antireflecting film system (1300 Å) (a); experimental dependencies of reflection of fianite film on Si and Ge (b).

The experimental dependences of enlightenment (the dependence of reflectance on the wavelength) of cubic zirconia films on Si and Ge, (Ge on their optical properties similar to GaAs) exhibit excellent antireflective properties of cubic zirconia (Fig. 23 b). As is evident from the graphs, the minimum reflection can drop to 0-1, 5%. Position of the minimum depends on the thickness of the film. When it gets thinned twice the minimum would be in the solar spectrum. Plateau in the curve shows the reflection from the back side of the substrate in the transmission range for Si. So the gain due to the use of antireflecting fianite film reaches 20-30%.

So, it was experimentally proved that in case of use of 1300 Å thick fianite film, reflection may actually fall to zero in the wavelength range $\lambda = 1.06 - 1.54 \mu\text{m}$.

A new, non-standard, fianite use as a reflecting film (in contrast to anti-reflective film!) was proposed. Such unexpected application may appear useful for screening of peripheral (non-photosensitive) photodetector areas. For standard screening of such areas, forming of proper photosensitive areas, metallic masks sputtered to SiO_2 have been used. But such solution causes notable spurious capacitance of the metal-oxide-semiconductor structure; provided that such capacities are inadmissible in a number of photodetectors, in particular – in high frequency photodetectors. In case of screening by the reflecting oxide (for this purpose the thickness should be chosen as $W = 1/2 \lambda n_{\text{ok}}$), no surface capacity is being formed, of cause; spurious capacitance is absent. In such case, fianite film may reflect about 60% of radiance from the surface.

5.2 Silicon solar cells with fianite antireflecting layer

Experimental dependencies of antireflection of fianite films deposited on commercial solar cells were recorded. The reflection spectra of fianite obtained on two such samples are shown in Fig. 25a. The plots (Fig. 24) demonstrate excellent antireflecting properties of the fianite films. The plots also apparently demonstrate that the reflection drops to 0 – 1.5 % in the minima. A position of the minimum depends on the film thickness. At the film thinning the minimum occurs in the solar spectrum. Therefore, energy gain due to the application of the antireflecting fianite films approaches to 20-30%.

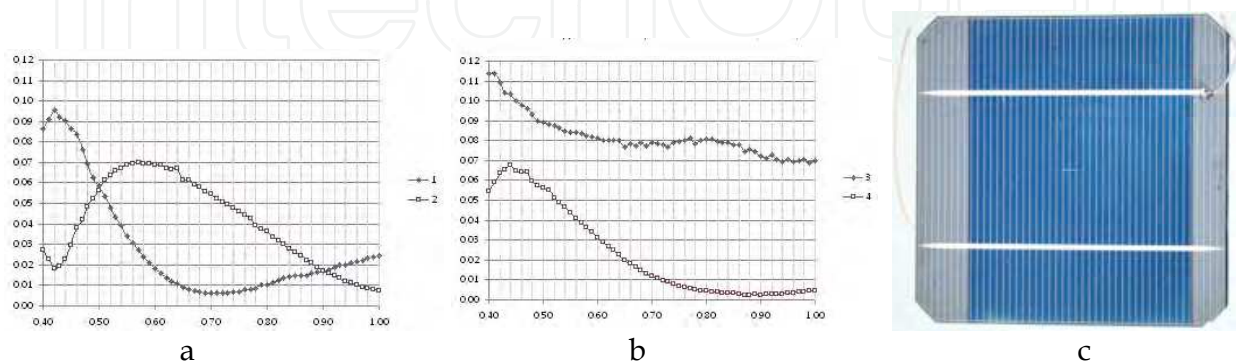


Fig. 24. Antireflecting properties of fianite films of 580 Å (a) and 1050 Å (b) thickness obtained on the industrial items (c) of Si solar cells of 4" x 4" size.

5.3 New ecologic technique of formation of *p-n* junctions in Si for solar sells

The majority of modern technologies of semiconductor devices are based on generation of different conductivity areas in the semiconductor and in particular of *p-n* junctions. For this purpose the crystals are doped, by means of three basic processes: diffusion, ion implantation, and irradiation. The donor and acceptor impurities coexist in real silicon crystals. Therefore there is an alternative possibility: to redistribute available impurities to fabricate the areas of different conductivity type. Traditional doping-based techniques (diffusion, ion implantation, a radiating doping) have the common drawbacks such as : (1) high temperatures of the processing. The diffusion doping is usually carried out at the temperature higher than 1100°C. After ion or radiating doping the subsequent high temperature annealing of the radiation defects should be carried out; (2) undesirable contamination of the crystal by new impurities could occur; (3) nearly all dopants are poisonous, leading to contamination of the environment. In the present work we consider a new technique of formation of *p-n* junctions in silicon, which provides facilitation and cost reduction of production process of semiconductor devices such as solar cells.

5.4.1 Experimental

The *p*-Si wafers were cut from boron-doped CZ crystals of various resistivities (with the boron concentration about 10^{15} cm⁻³). The wafers were irradiated by 1–5 keV Ar ions in a gas discharge plasma. Then the wafers were cleaved, and the depth profile of the conductivity type was inspected by SEM-EBIC (scanning electron microscopy-electron beam induced current) technique. For this purpose, a high quality Schottky barrier was made by metal coating. This process resulted in formation of an *n-p* junction at some depth, which is clearly revealed as a sharp peak of EBIC signal (Fig. 25).

The formation of an n -type region below the irradiated surface was also confirmed by a conventional thermo-probe technique. Upon increasing the irradiation time, the depth of the n - p junction (denoted by X_d) increases (Fig. 26). Some n -type (phosphorus-doped) wafers were also irradiated and inspected; in this case no p - n junction was found [61, 62]. The junction depth X_d is a non-linear function of the irradiation time t . No junction was found in reference non-irradiated wafers. There is some "dead" time (1–15 min) in the junction propagation. After prolonged irradiation, the junction reaches some final position (Fig. 26 b) that can be quite close to the back (non-irradiated) surface of the wafer. In some range of duration (neither too short nor too long) the depth is roughly proportional to $t^{1/2}$ – a typical dependence for a diffusion process.

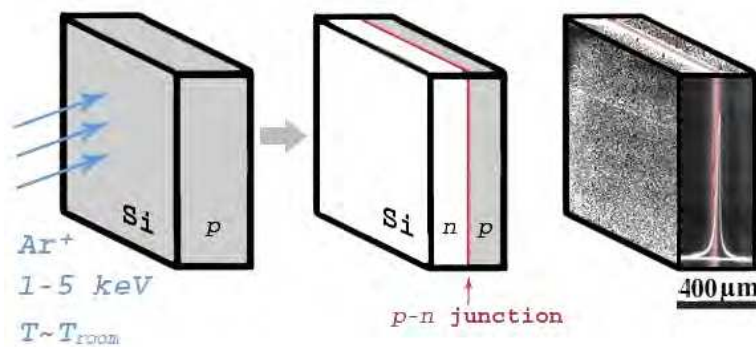


Fig. 25. Scheme of experiment

Peculiarities of n - p junction propagation. The n - p junction propagation was found to be sensitive to the state of the wafer surface. If the irradiated surface is bright polished, the junction moves faster, in comparison to the abrasion-polished surface. The surface defects, like scratches, cause a local distortion of the junction shape. The scratches at the backside 'attract' the junction. On the contrary, near the wafer edges, the junction propagation is retarded (Fig. 27). Striation non-uniformity of Si affects the shape of inversion p - n junction too (Fig. 28).

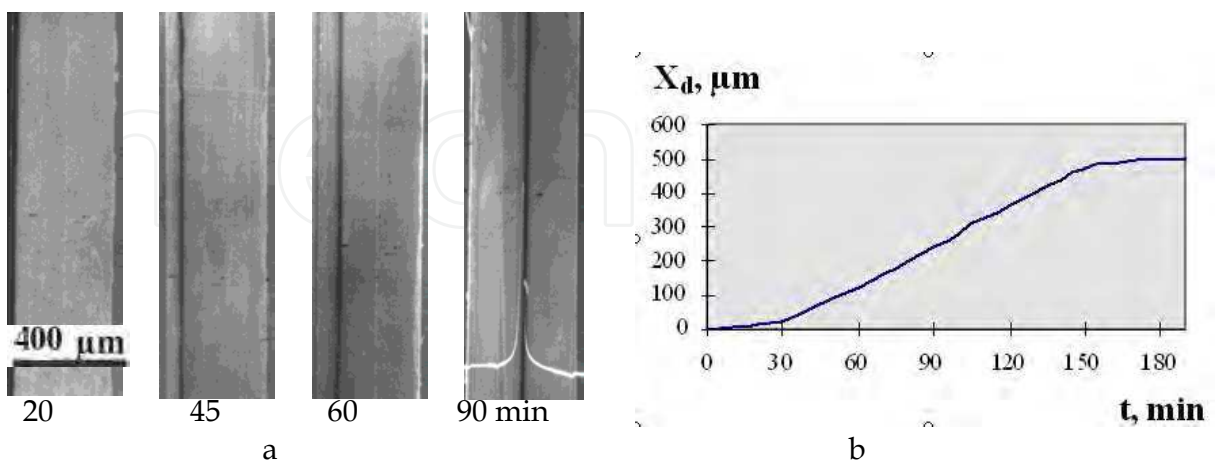


Fig. 26. SEM microphotograph made both in secondary emission and EBIC modes of inversion p - n junctions on a cleaved Si wafer (a). The wafers were irradiated at the left side. The dark vertical strip is the image of p - n junction. The p - n junction depth X_d in dependence of the time of exposure to Ar ions (b).

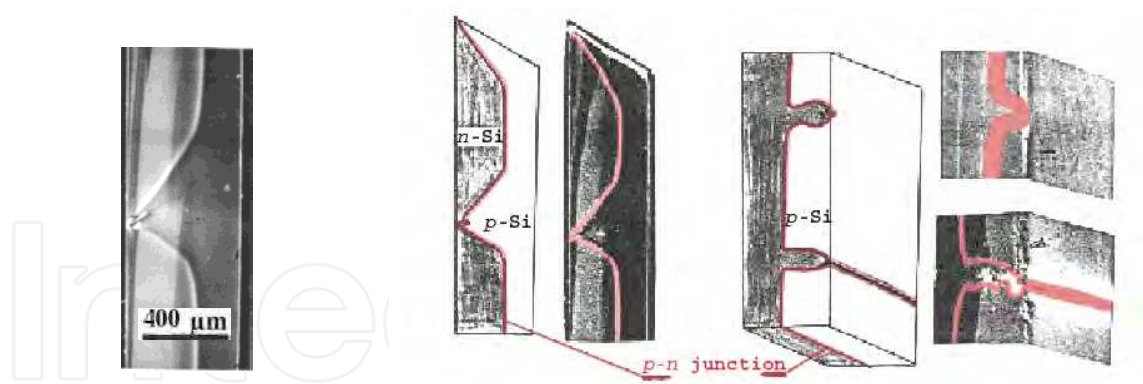


Fig. 27. Influence of surface damage in Si wafer on the shape of inversion p - n junction

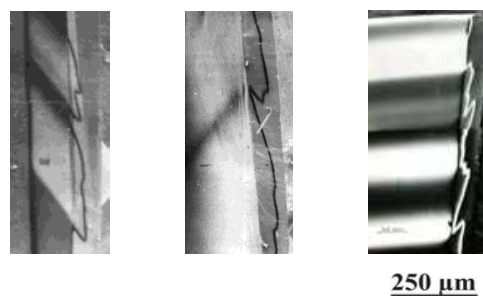


Fig. 28. Influence of non-uniformity of Si wafer on the form of inversion p - n junction

These results indicate to the role of the irradiation-induced self-interstitials: the local self-interstitial concentration is sensitive to the sinking ability of the sample surface. Particularly, the scratches at the backside may get the surface impurities from the adjacent regions of the surface, thus improving the sinking ability of those regions.

One can argue that the p - n inversion is caused by some fast-diffusing donor impurity introduced during Ar irradiation. To check this possibility, we used the secondary-ion mass-spectrometry. An irradiated sample with a shallow p - n junction and a reference non-irradiated sample were inspected using layer-by-layer etching. No difference in the impurity content between the two samples was found which proves that the irradiation did not lead to any contamination of the sample near the surface.

It is therefore accepted that the p - n inversion is caused by in-diffusion of intrinsic point defects (self-interstitials) which leads to a loss of boron acceptors by kicking out the boron atoms B_s into the interstitial state B_i . The B_i atoms are known to be donors in p -Si [63]. Most likely, B_i will be paired to B_s , into neutral B_iB_s defects. The conductivity will then change to n -type, due to either isolated B_i or due to residual donors (phosphorus and grown-in thermal donors) that are present already in the initial state, before the irradiation.

The thermal donors are well known to be produced by a heat treatment around 450°C , and to be annihilated by annealing at $T > 600^\circ\text{C}$. It was found that after several hours at 450°C , the n - p junction persisted. However, after one hour at 750°C the p - n junction disappeared. This result can be treated as an indication of role of the thermal donors. On the other hand, it can be attributed to conversion of B_i back into B_s by annealing at higher T .

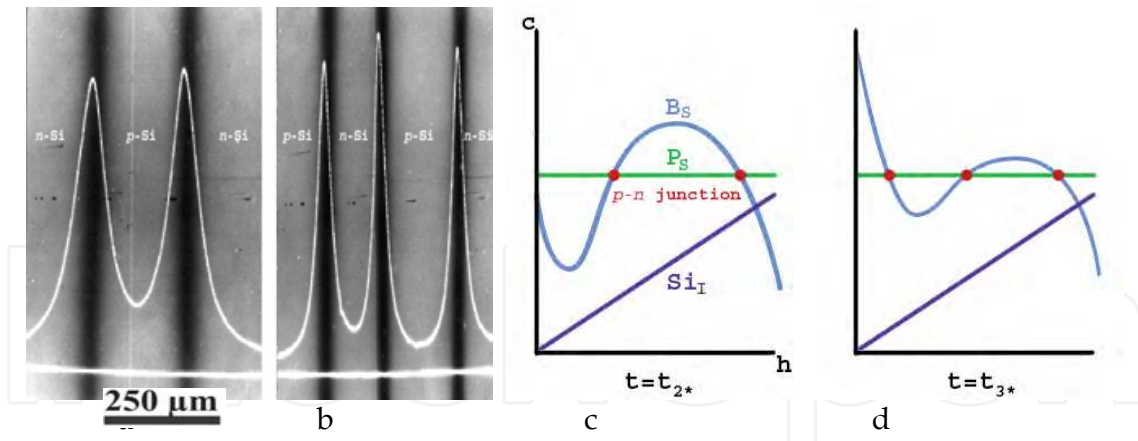


Fig. 29. Schematic profiles of self-interstitials and substitutional boron after irradiated at the front side (a) and back side (b), the horizontal line shows the zero level; model of the depth profile of the SEM-EBIC signal for a sample with two (c) and three (d) irradiation-induced p-n junctions.

By varying the irradiation conditions (for instance, using a two-side irradiation), multiple junctions can be produced. An example of a double and a triple junction is shown in Fig. 29.

5.4.2 Model

A proposed mechanism of this process consists mainly in the following [64]. The irradiation of the sample by inert ions generates a flux of silicon interstitial atoms Si_I directed from a surface in the bulk of the sample. Due to very high diffusivity of Si_I [65] (even at low temperatures), the steady non-uniform distribution of Si_I in a sample is formed (Fig. 30 a). Equilibrium concentration Si_I at low temperatures is very low, therefore a huge supersaturation of Si_I is created, which results in a sharp increase in the boron interstitial component, B_i . Reaction of kicking-out boron and the backward reaction ($B_i \rightarrow B_s + Si_I$) establish dynamically equilibrium ratio between B_i and Si_I . This ratio is proportional to the supersaturation of Si_I . Therefore the loss of boron acceptors will be more pronounced in the wafer part with a higher concentration Si_I . As a result the local inversion of conductivity occurs in this part. This model implies that the self-interstitials diffuse very fast at low T (below 100 °C), and penetrate to the depth of at least 300 μm within 100 min (Fig. 30b). Accordingly the self-interstitial diffusivity, at the irradiation temperature, is at least as high as $10^{-7} \text{ cm}^2/\text{s}$.

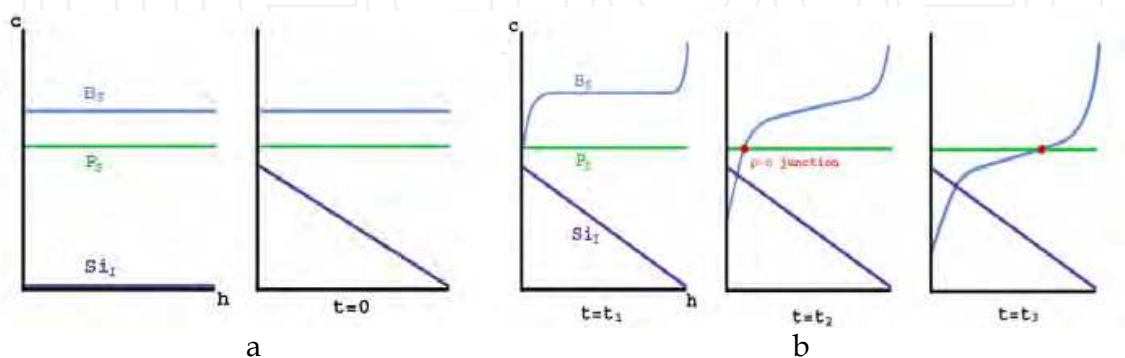


Fig. 30. Schematic profiles of self-interstitials and substitutional boron in the beginning of the process (a) and at successive time of intermediate stage of junction propagation (b).

In the subsequent discussion, we concentrate on the boron acceptor loss, assuming that the near-surface region contains some concentration of donors, N_d , which is less than the initial concentration of the boron acceptors, N_o .

A change in the substitutional boron concentration, due to the kick-out reaction (and due to the inverse reaction of kicking out the silicon lattice atoms by B_i), is described by a simple equation,

$$dN_s/dt = -\alpha (N_s C - KN_i) \quad (1)$$

where C is the local (depth-dependent) self-interstitial concentration, α is the kinetic constant of the direct kick-out reaction and K is the equilibrium constant in the mass-action law that relates the concentration for the case of equilibrium between the reacting species ($N_s C/N_i = K$). The highest self-interstitial concentration, C_f , is reached near the front surface; it is defined by the balance of the production rate (proportional to the Ar flux) and the consumption rate by local Ar-produced vacancies and by sinking of self-interstitials at the front surface. With specified C , the concentration ratio of the interstitial and substitutional boron species, N_i/N_s , tends to C/K due to the reaction (1). A strong loss of acceptors occurs if $C \gg K$. It is therefore assumed that this inequality holds at least at the front surface: $C_f \gg K$.

Initial stage of boron acceptor loss. At short irradiation time, the term KN_i in Eq. (1) is negligible, and the boron concentration near the front surface is lost exponentially,

$$N_s(t) = N_o \exp(-\alpha C_f t) \quad (2)$$

The n - p junction appears when N_s becomes less than N_d . This moment (t_d) lies experimentally, between 1 and 10 min. The product αC_f is estimated, from Eq. (2), to be in the range 0.01–0.001 s^{-1} .

Propagation of the n - p junction The near-surface region – where a large fraction of boron is already displaced into interstitial state B_i (and then paired into $B_i B_s$) – expands as more self-interstitials diffuse from the front surface into the bulk. The mass action law, $N_s C/N_i = K$, is valid at duration longer than the kick-out reaction time (10 min or less). The boron-depleted region corresponds, approximately, to the condition $C(x) > K$. At not too long duration, the self-interstitials penetrate to some limited depth (Fig. 30 b), and the n - p junction resides at some intermediate position within the sample. Finally, the $C(x)$ profile approaches a steady-state linear shape: the interstitials generated at the front surface are consumed at the back surface (Fig. 30 b). Therefore, the n - p junction does not reach the back surface but stops at some final position, just like observed.

The self-interstitial flux into the sample bulk is, approximately, DC_f/x_d , where x_d is the size of the boron-depleted region (x_d is almost identical to position X_d of the n - p junction). The total amount of the remaining boron is equal to $C_o(L-x_d)$, where L is the wafer thickness. The boron loss rate, dQ/dt , is twice as large as the above self-interstitial flux (each consumed Si_i leads to a loss of two B_s : one by kick-out, and the other by pairing of B_i to B_s). The following equation provides a solution for the junction depth $x_d(t)$,

$$x_d = (4DC_f t/N_o)^{1/2} \quad (3)$$

The DC_f product is estimated to be $5 \times 10^7 \text{ cm}^2 \text{ s}^{-1}$ from Eq. (3). Above, we estimated the product αC_f (where α is the kick-out kinetic coefficient). By these numbers, the α / D ratio is of the order of 10^{-10} cm . If the kick-out reaction were limited just by self-interstitial diffusion (which means

that any 'encounter' of a self-interstitial with the boron atoms immediately leads to the boron displacement into the interstitial state), the coefficient a/D ratio would be equal to $4\pi r = 4 \times 10^{-7}$ cm, where r is of the order of the interatomic distance. The difference between the two numbers indicates some kinetic barrier (roughly, 0.25 eV) for the kick-out reaction.

A possibility of long-range migration of interstitial boron. It was assumed in the above discussion that the boron atoms displaced into interstitial state do not diffuse much from the initial location. The alternative possibility is that the B_i species are of high mobility (comparable to the self-interstitial mobility), and therefore they can migrate to the distance comparable to the sample thickness. In this case, a considerable spatial redistribution of boron impurity would occur. The final profile of B_i would be smoothed by diffusion to some constant (depth-independent) concentration N_i . The mass-action law would then imply that the substitutional boron concentration, $N_s = N_i K/C$, is inversely proportional to $C(x)$. Therefore, substitutional boron would accumulate near the back surface, where $C(x)$ is at minimum. Such a profile of substitutional impurity (with a well-pronounced accumulation at the back surface) is typical during in-diffusion of Au and Pt impurities [65, 66].

A formation of triple junction (Fig. 29 b) can be accounted for by the long-distance migration of B_i . The boron profile after the first irradiation is of the type shown in Fig. 30 b ($t=t_2$), with just one junction. The second (back-side) irradiation creates an n -region near the back surface, and also results in the boron acceptor accumulation near the front side (now non-irradiated). Then a region adjacent to the front side becomes again of p -type conductivity. The resulting structure is $p-n-p-n$ (Fig. 29b, d).

5.4.3 Application of solar and the other

Due to physical nature and peculiarities of generation of the inverse $p-n$ junction its application is the easiest and the most efficient in those semiconductor technologies, which involve the development of two-dimensional (flat) $p-n$ transitions over a considerable square [67]. Solar cells are related to the devices of such a type. Further development of these investigations will lead to the new technology of $p-n$ junction formation in silicon, providing simplification and cost reduction of production process of solar cells and another various semiconductor devices.

5.5 The development of III-V heterostructures for solar cells

The following four types of heterostructures based on InGaAsP compounds have been developed for solar cells by means of MOCPE using Aixtron AIX 200RF installation and capillary epitaxy technique under improved conditions and by using the refined technologies of the epitaxial growth on GaAs substrates of n - and p -types of conductivity:

1. p -GaAs substrate, 2.7 μm absorption range, InGaP window - 0.2 μm , contacting layer GaAs - 0.2 μm ;
2. p -GaAs substrate, InGaP barrier layer - 0.03 μm , 3 μm - GaAs absorption range, InGaP window - 0.06 μm , contacting layer - 0.6 μm ;
3. n^+ - GaAs substrate, barrier InGaP - 0.2 μm , absorption range - undoped GaAs 3 μm , emitter - p -GaAs - 0.4 μm , p -InGaP window - 0.02 μm , contacting layer p -GaAs - 0.4 μm ;
4. n^+ - GaAs substrate, buffer n^+ -GaAs-0.6 μm ; barrier n^+ -InGaP-0.05 μm ; absorption layer undoped GaAs-3.3 μm ; emitter p^+ -GaAs-0.07 μm ; window p^+ - InGaP-0.07 μm ; contacting layer p^{++} -GaAs-0.2 μm ; antireflecting layer fianite-0.1 μm ;

Prototypes of the solar cells have been manufactured using the obtained samples. Fianite films were used as antireflecting and protective coatings [68, 69]. The films were deposited by means of magnetron sputtering (Fig. 31).

The study of characteristics of the prototypes of the heterostructure solar cell has shown 20-30 % efficiency gain due to the application of the fianite antireflecting films.

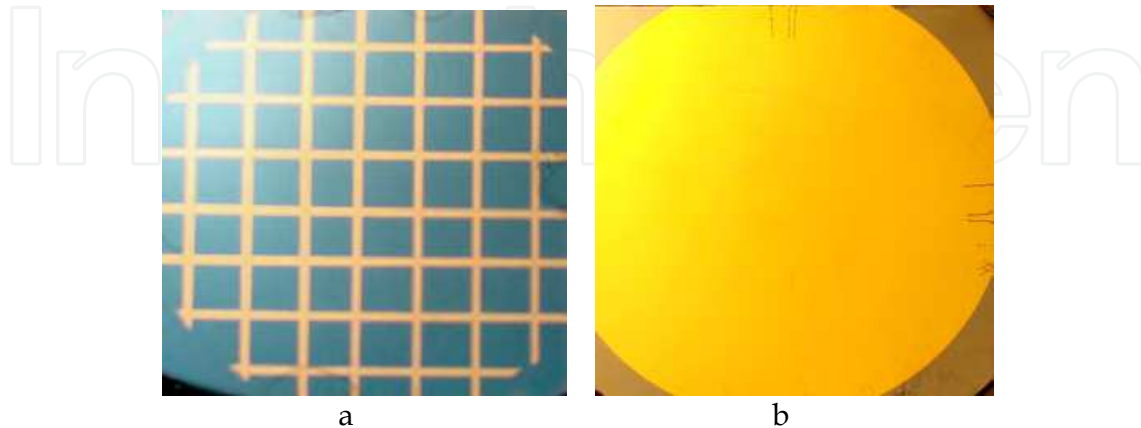


Fig. 31. Prototype sample of the heterostructure solar cell of 40x40 mm size supplied with fianite antireflecting coating: functional side with Au contacting routs (a), reverse side with Au+Ti contacting layer (b)

6. Conclusions

The unique properties of fianite as monolithic substrate and buffer layer for Si, Ge and $A^{III}B^V$ compounds epitaxy; protecting, stabilizing and antireflecting coatings, as well as a gate dielectric in photosensitive opto-electronic devices have been demonstrated. The results obtained in this work have actually demonstrated advantages of fianite as novel multipurpose material for new optoelectronics technologies.

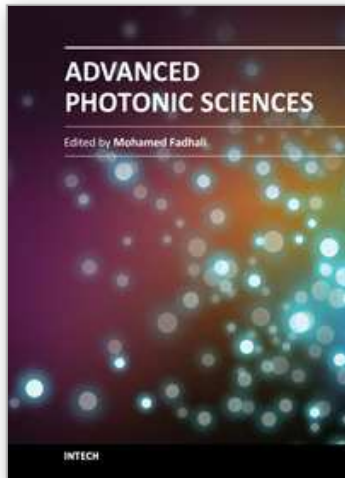
7. References

- [1] V.I. Aleksandrov, V.V. Osiko, A.M. Prokhorov, V.M. Tatarintsev. New technique of the synthesis of refractory single crystals and molten ceramic materials. Vestnic AN SSSR №12 (1973) 29-39. (in Russian)
- [2] V.I. Aleksandrov, V.V. Osiko, V.M. Tatarintsev, A.M. Prokhorov. Synthesis and crystal growth of refractory materials by RF melting in a cold container. Current Topics in Materials Science. 1 (1978) 421-480.
- [3] E.E. Lomonova, V.V. Osiko: Growth of Zirconia Crystals by Skull-Melting Technique. In: Crystal Growth Technology. Ed. by H.J. Scheel and T. Fukuda (John Wiley @ Sons, Chichester, England 2003) pp. 461-484
- [4] Yu.S. Kuz'minov, E.E. Lomonova, V.V. Osiko Cubic zirconia and skull melting Cambridge International Science Publishing Ltd., UK, 346 pp. 2009
- [5] V.V.Osiko, M.A.Borik, E.E.Lomonova Synthesis of refractory materials by skull melting technique. Handbook of Crystal Growth, Springer, 2010, p.433-469.
- [6] I. Golecki, H.M. Manasevit, L.A. Moudy, J.J. Yang, and J.E Mee. Heteroepitaxial Si films on yttria-stabilized, cubic zirconia substrates. // Appl. Phys. Lett., 1983, v. 42, No. 6, p. 501-503.

- [7] D. Pribat, L.M. Mercandalli, J. Siejka, J. Perriere Interface oxidation of epitaxial silicon deposits on (100) yttria stabilized cubic zirconia, *J.Appl.Phys.* 58, 313-320 (1985)
- [8] L.M. Mercandalli, D. Diemegand, M. Crose, Y. Sierka. Recent progress in epitaxial growth of semiconducting materials on stabilized zirconia single crystals, *Proc.Soc.Photo-Opt. Istr.Eng.* 623, 133-210 (1986)
- [9] V.G. Shengurov, V.N. Shabanov, A.N. Buzynin, et al., *Mikroelektronika*, no. 6 (1996) 204.
- [10] A.N. Buzynin, V.V. Osiko, E.E. Lomonova, Yu.N. Buzynin, A.S. Usikov. Epitaxial films of GaAs and GaN on fianite substrate. // *Wide-Bandgap semiconductors for High Power, High Frequency and High Temperature.* (Mat. Res. Soc. Simp. Proc. 1998). Vol.512, Pittsburg, PA, p. 205-210.
- [11] A.N. Buzynin, V.V. Osiko, Yu.K. Voron'ko, et al. // *Izv. Akad. Nauk, Ser. Fiz.* 69 (2005) 211.
- [12] P.A. Anderson, C.E. Kendrick, R.J. Kinsey, et. al. (111) and (100) YSZ as substrates for indium nitride growth. // *Physica status solidi (c)*, 2005, v. 2, N.7, p. 2320 - 2323.
- [13] Y.Z. Yao-Zhi Hu, S.P. Sing-Pin Tay, *J. Vac. Sci. Technol. B* 19 (2001) 1706.
- [14] S.J. Wang, C.K. Ong, S.Y. Xu, et al. Electrical properties of crystalline YSZ films on silicon as alternative gate dielectrics, *Semicond. Sci. Technol.* 16, L13-L16 (2001)
- [15] S.J. Wang, C.K. Ong. Rapid thermal annealing effect on the electrical properties of crystalline YSZ gate dielectrics. // *Semiconductor Science and Technology*, 2003, v. 18, p. 154-157.
- [16] A.N. Buzynin, V.V. Osiko, E.E. Lomonova, et. el. Epitaxial films of III-V compound on fianite substrates. // *Proc. of International Congress on Advanced Materials, their Processes and Applications*, 25-28 September 2000, Munich, Germany, Article 672.
- [17] A.N. Buzynin, V.V. Osiko, Yu.N. Buzynin, B.V. Pushnyi. Growth of GaN on fianite by MOCVD capillary epitaxy technique. // *MRS Internet Journal of Nitride Semiconductor Research.* 1998, Vol.4, Article 49. (<http://nsr.mij.mrs.org/4/49/>).
- [18] A.N. Buzynin, V.V. Osiko, Yu.N. Buzynin et al. // *Izv. Ross. Akad. Nauk, Ser. Fiz.*, 2002, v. 66, n. 9, p. 1345-1350.
- [19] A.N. Buzynin, V.V. Osiko, E.E. Lomonova, Yu.N. Buzynin, A.S. Usikov. Epitaxial films of GaAs and GaN on fianite substrate. // *Wide-Bandgap semiconductors for High Power, High Frequency and High Temperature.* (Mat. Res. Soc. Simp. Proc. 1998). Vol.512, Pittsburg, PA, p. 205-210.
- [20] R. Paszkiewicz, B. Paszkiewicz, R. Korbutowicz, et al, MOVPE GaN Grown on Alternative Substrates // *Cryst. Res. Technol.* 2001, v.36, N 8-10, p. 971-977.
- [21] P.D.C. King, T.D. Veal, S.A. Hatfield, et. al. X-ray photoemission spectroscopy determination of the InN/yttria stabilized cubic-zirconia valence band offset. // *Appl. Phys. Let.*, 2007, v. 91, p. 112103-1 - 112103-3.
- [22] T. Nakamura, Y. Tokumotoa, R. Katayamaa, et. al. RF-MBE growth and structural characterization of cubic InN films on yttria-stabilized zirconia (001) substrates. // *J. of Crystal Growth*, v. 301-302, April 2007, p. 508-512.
- [23] A.N. Buzynin and V.P. Kalinushkin, Laser characterization of sapphire defectts. *Proc. of Inter. Congress" Materials Week-2001": Advanced Materials, their Processes and Applications*, 1-4 October 2001, Munich, Germany, Article 389.
- [24] A.N. Buzynin and V.P. Kalinushkin New technique of laser characterization of sapphire and fianite crystals // *Abstracts of the Laser Interaction with Matter International Symposium" (LIMIS2010)*, Aug. 15th to 18th, 2010, Changchun, China.
- [25] G.G. Shahidi. SOI technology for the GHz era. // *IBM J. of Research and Development*, 2002, v.46, No. 2/3, p. 121-132.

- [26] A.N. Buzynin, V.V. Osiko, Yu.N. Buzynin, et al. // *Bulletin of the Russian Academy of Sciences: Physics* 74 (2010) 1027-1033
- [27] N.N. Sheftal and A.N. Buzynin// *Vestnik Moscow Univ.* 3 (1972) 102; *Nat. Trans. Cent. The Yohn Crenan Library, 35w, 33rd St., Chicago IL 60616 USA.*
- [28] Smith, H. I.; Flanders, D. C.// *Appl. Phys. Lett.* 1978, 32, 349.
- [29] Masatomo Sumiya, Youichi Kurumasa, Kohji Ohtsuka, et al., *J. Cryst. Growth*, vol. 237 – 239 (2002) 1060.
- [30] E.I. Rau, A.N. Zhukov, E.B. Yakimov, // *Solid-State Phenomena* 1998, v. 327, p. 53–54.)
- [31] A.N. Buzynin, Yu.N. Buzynin, A.V. Belyaev, A.E. Luk'yanov, E.I. Rau. Growth and defects of GaAs and InGaAs films on porous GaAs substrates. // *Thin Solid Films* 2007, v. 515, p. 4445–4449.
- [32] G.G. Shahidi. SOI technology for the GHz era. // *IBM J. of Research and Development*, 2002, v.46, No. 2/3, p. 121–132.
- [33] S.J. Wang, C.K. Ong, S.Y. Xu, P. Chen, W.C. Tjiu, J.W. Chai, C.H. Huan, W.J. Yoo, J.S. Lim, W. Feng, W.K. Choi Crystalline zirconia oxide on silicon as alternative gate dielectrics, *Appl. Phys. Letters* 78, 1604-1606 (2001)
- [34] S.J. Wang, C.K. Ong, S.Y. Xu, P. Chen, W.C. Tjiu, A.C.H. Huan, W.J. Yoo, J.S. Lim, W. Feng, W.K. Choi Electrical properties of crystalline YSZ films on silicon as alternative gate dielectrics, *Semicond. Sci. Technol.* 16, L13-L16 (2001)
- [35] T. Ngai, W.J. Qi, R. Sharma, J. Fretwell, X. Chen, J.C. Lee, S. Banerjee Electrical properties of ZrO₂ gate dielectric on SiGe, *Applied Physics Letters* 76, 502-504 (2000)
- [36] S. Abermann, G. Pozzovivo, J. Kuzmik et al MOCVD of HfO₂ and ZrO₂ high-*k* gate dielectrics for InAlN/AlN/GaN MOS-HEMTs. // *Semicond. Sci. Technol.*, 2007, v. 22, p. 1272–1275
- [37] H. Fukumoto, T. Imura and Y. Osaka. Heteroepitaxial growth of yttria-stabilized zirconia on silicon // *Jpn. J. Appl. Phys.*, 1988, v.27, No.8, p. L1404–L1405
- [38] T. Hata, K. Sasakia, Y. Ichikawa and K. Sasakia. Yttria-stabilized zirconia (YSZ) heteroepitaxially grown on Si substrates by reactive sputtering. // *Vacuum*, 2000, v.59, issues 2-3, p. 381-389
- [39] A.N. Buzynin, V.V. Osiko, V.V. Voronov, Yu.N. Buzynin et al. Epitaxial Fianit films on Si and GaAs. // *Bulletin of the Russian Academy of Sciences. Physics.*, 2003, v.67, No 4, p.586–587
- [40] V.G. Beshenkov, A.G. Znamenskii, V.A., Marchenko et al. Widening temperature range of epitaxial growth of YSZ films on Si [100] Расширение области температур эпитаксиального роста пленок YSZ на Si [100] under magnetron sputtering. // *Journal of technical physics*, 2007, v.77, N5, p. 102–107
- [41] J.M. Vargas, P. Brown, T. Khan et. al. Superconducting half-wave microwave resonator on YSZ buffered Si(100). // *Applied Superconductivity*, 2001, v. 11, N. 1, p.392 – 394
- [42] C. A. Copetti, H. Soltner, J. Schubert, et. al. High Quality Epitaxy of YBa₂Cu₃O_{7.5} on Silicon- on-sapphire with the Multiple Buffer Layer YSZ/CeO₂. *Applied Physics Letters*, 1993, v. 63, N 10, p.1429-1431
- [43] T. Khan, P. Brown, Yu. Vlasov et al. YBa₂Cu₃O₇ on Sputter Deposited ZrO₂ Buffered (100) Si - Processing and Characterization," *Advances in Cryogenic Engineering (Materials)*, 2000, v. 46, p. 901-905
- [44] J. Sanghun; T. Matsuda; U. Akira; W. Kiyotaka; I. Yoko; H. Hyunsang; Interfacial properties of a hetero-structure YSZ/p-(100)Si prepared by magnetron sputtering. *Vacuum*, 2002, vol. 65, n°1, p. 19 - 25
- [45] N. Wakiya, T. Yamada, K. Shinozaki, and N. Mizutani: Heteroepitaxial growth of CeO₂ Thin Film on Si(001) with an Ultra Thin YSZ Buffer Layer. *Thin Solid Films*, 2000, v.371, p.211-217.

- [46] S. Kaneko, K. Akiyama, T. Ito et. al. Single domain epitaxial growth of yttria-stabilized zirconia on Si (111) substrate. // *Ceramics International*, 2008, article in press.
- [47] R. Lyonnet, A. Khodan, A. Barthe'le'my, et al. Pulsed laser deposition of $Zr_{1-x}Ce_xO_2$ and $Ce_{1-x}La_xO_{2-x/2}$ for buffer layers and insulating barrier in oxide heterostructures. // *J. of Electroceramics*, 2000, 4, No. 2/3, p. 369-377
- [48] N. Pryds, B. Toftmann, J.B. Bilde-Sørensen et al. Thickness determination of large-area films of yttria-stabilized zirconia produced by pulsed laser deposition *Applied Surface Science*, 2006, v. 252, issue 13, p. 4882-4885
- [49] A.P Caricato., G.A. Barucca, Di. Cristoforo et al. Excimer pulsed laser deposition and annealing of YSZ nanometric films on Si substrates // *Applied Surface Science*, 2005, v. 248, issues 1-4, p. 270 - 275
- [50] Sang-Chul Hwang and Hyung-Shik Shin. Effect of Deposition Temperature on the Growth of Yttria-Stabilized Zirconia Thin Films on Si(111) by Chemical Vapor Deposition. // *J. of the American Ceramic Society*, 1999, v. 82, issue 10, p 2913-2915
- [51] A. Osinsky, S. Gangopadhyay, J. W. Yang, et al. // *Appl.Phys.Lett.* 72 (1998) 561
- [52] M. F. Wu, A. Vantomme and G. Langouche, B. S. Zhang and Hui Yang, *Appl.Phys.Lett.* 80 (2002) 4130
- [53] Supratik Guha and Nestor A. Bojarczuk, *Appl.Phys.Lett.* 72 (1998) 415
- [54] Lianshan Wang, Xianglin Liu, Yude Zan, Jun Wang, Du Wang, Da-cheng Lu, and Zhanao, *Appl.Phys.Lett.* 72 (1998) 109
- [55] N. P. Kobayashi," J. T. Kobayashi, P. D. Dapkus," W.-J. Choi, and A. E. Bond, *Appl.Phys.Lett.* 71 (1997) 3569
- [56] A. Ohtani, K. S. Stevens, and R. Beresford, *Appl.Phys.Lett.* 65 (1994) 61
- [57] A.J. Steckl, J. Devrajan, C. Tran and R. A. Stall, *Appl.Phys.Lett.* 69 (1996) 2264
- [58] Y.Z. Yao-Zhi Hu, S.P. Sing-Pin Tay, *J. Vac. Sci. Technol. B* 19 (2001) 1706
- [59] A.N. Buzynin, T.N. Grishina, T.V. Kiselyov, et al. Zirconia-based Solid Solutions – New Materials of Photoelectronics. // *Optical Memory & Neural Networks (Information Optics)*. № 4, 2009, p.323-331
- [60] A.N.Buzynin, E.E.Lomonova, T.N.Grishina, et al. Semiconducting photosensitive structures with passivating protective zirconia coating. // *Applied physics*. № 2. 2009, p. 105-109
- [61] A.N. Buzynin, A.E. Luk'yanov, V.V. Osiko, V.V. Voronkov, *Mater. Res. Soc. Proc.* (Pittsburg, PA) 378 (1995) 653.
- [62] A.N. Buzynin, A.E. Luk'yanov, V.V. Osiko, V.V. Voronkov, *Mater. Res. Soc. Proc.* (Pittsburg, PA) 510 (1998).
- [63] R.D.Harris, J.L.Newton and G.D.Watkins, *Phys.Rev. B* 36, 1094 (1987).
- [64] A.N.Buzynin, A.E.Luk'yanov, V.V.Osiko, V.V.Voronkov. *Nuclear Instrum. and Methods in Physics Research, B* 186 (2002), p.366-370.
- [65] N.A. Stolwijk, J. Holzl, W. Frank, E.R. Weber, H. Mehrer, *Appl. Phys. A* 39 (1986) 37.
- [66] H. Zimmermann, H. Ryssel, *Appl. Phys. A* 55 (1992) 121.
- [67] Patent "Metod of p-n junction formation in silicon", № RU 2331136 C2., 10.08.2008.
- [68] A.N. Buzynin, V.V. Osiko, Yu.N. Buzynin, et al Fianite: a multipurpose electronics material // *Bulletin of the Russian Academy of Sciences: Physics*, 2010, Vol. 74, No. 7, pp. 1027-1033.
- [69] A.N. Buzynin, Yu.N. Buzynin, V.V. Osiko, et al Antireflection fianite and ZrO_2 coatings for solar cells // *Bulletin of the Russian Academy of Sciences: Physics*, 2011, Vol. 75, No. 9, 1213-1216.



Advanced Photonic Sciences

Edited by Dr. Mohamed Fadhalli

ISBN 978-953-51-0153-6

Hard cover, 374 pages

Publisher InTech

Published online 21, March, 2012

Published in print edition March, 2012

The new emerging field of photonics has significantly attracted the interest of many societies, professionals and researchers around the world. The great importance of this field is due to its applicability and possible utilization in almost all scientific and industrial areas. This book presents some advanced research topics in photonics. It consists of 16 chapters organized into three sections: Integrated Photonics, Photonic Materials and Photonic Applications. It can be said that this book is a good contribution for paving the way for further innovations in photonic technology. The chapters have been written and reviewed by well-experienced researchers in their fields. In their contributions they demonstrated the most profound knowledge and expertise for interested individuals in this expanding field. The book will be a good reference for experienced professionals, academics and researchers as well as young researchers only starting their carrier in this field.

How to reference

In order to correctly reference this scholarly work, feel free to copy and paste the following:

Alexander Buzynin (2012). Fianite in Photonics, Advanced Photonic Sciences, Dr. Mohamed Fadhalli (Ed.), ISBN: 978-953-51-0153-6, InTech, Available from: <http://www.intechopen.com/books/advanced-photonic-sciences/fianite-in-photonics>

INTECH
open science | open minds

InTech Europe

University Campus STeP Ri
Slavka Krautzeka 83/A
51000 Rijeka, Croatia
Phone: +385 (51) 770 447
Fax: +385 (51) 686 166
www.intechopen.com

InTech China

Unit 405, Office Block, Hotel Equatorial Shanghai
No.65, Yan An Road (West), Shanghai, 200040, China
中国上海市延安西路65号上海国际贵都大饭店办公楼405单元
Phone: +86-21-62489820
Fax: +86-21-62489821

© 2012 The Author(s). Licensee IntechOpen. This is an open access article distributed under the terms of the [Creative Commons Attribution 3.0 License](#), which permits unrestricted use, distribution, and reproduction in any medium, provided the original work is properly cited.

IntechOpen

IntechOpen